Table S1. List of literature affinities and references.

Name	Sequence	K_d Range (μM)
NFATc1	ALE**SPRIEIT**SCLG	2.5[1]-25[a,2]
NFATc2	SGL**SPRIEIT**PSHE	6[3]
AKAP79	RME**PIAIIIT**DT	0.4-1.5[4]
RCAN	T**PSVVVH**VC	1-45[3,5]
PVIVIT	AGPH**PVIVIT**GPHEE	0.5[4]
A238L	FKKK**PKIIIT**GCE	0.8[6]

Notes: a. Value reported as IC_{50}

Table S2. List of "triplicate low" peptides and fit parameters.

Sequence	Code	K_d (μM)	K_d (μM) Error
AGPHPVIVITGPHEE	1	1.713	0.091
SCRAMBLED	2	586.000	349.142
AGPHPVIVINGPHEE	4	58.021	3.840
AGPHPVIAVTGPHEE	5	230.516	63.064
AGPHPAIVITGPHEE	6	2.833	0.131
AGPHPAIVITGPHEE	7	1.780	0.067
AGPHPVIVITGPHEE	12	2.944	0.188
SCRAMBLED	13	352.219	133.781
AGPHPVIVVTGPHEE	14	1.784	0.115
AGPHPVIVINGPHEE	15	64.513	6.260
AGPHPVIAVTGPHEE	16	364.354	134.084
AGPHPAIVITGPHEE	17	2.701	0.098
AGPHPAIVITGPHEE	18	2.375	0.088
AGPHPVIVITGPHEE	23	2.665	0.150
SCRAMBLED	24	367.611	146.316
AGPHPVIVVTGPHEE	25	2.326	0.148
AGPHPVIVINGPHEE	26	50.276	1.826
AGPHPVIAVTGPHEE	27	358.745	96.248
AGPHPAIVITGPHEE	28	2.833	0.102
AGPHPAIVITGPHEE	33	1.736	0.103
PALESPRIEITSCLGL	34	99.399	14.722
ASGLSPRIEITPSHEL	35	4.361	0.170
ATDTTPSVVVHVCESD	37	262.428	90.082
KRMEPIAIIITDTEIS	38	19.812	1.546
PALESPRIEITSCLGL	39	105.503	16.398
ASGLSPRIEITPSHEL	40	10.442	0.538
ATDTTPSVVVHVCESD	42	256.631	81.701
KRMEPIAIIITDTEIS	43	25.145	2.325
PALESPRIEITSCLGL	44	138.115	30.674
ASGLSPRIEITPSHEL	45	3.726	0.114
ATDTTPSVVVHVCESD	47	296.430	122.092
KRMEPIAIIITDTEIS	48	27.232	2.167

Table S3. List of "triplicate high" peptides and fit parameters. X: phosphoserine, Z: phosphothreonine.

Sequence	Code	K_d (μM)	K_d (μM) Error
HPVIVITGPH	1	0.971	0.087
SCRAMBLED	2	1158.521	1164.153
HPVIVINGPH	4	26.769	1.586
HPVIAVTGPH	5	275.538	101.803
HAVIVITGPH	6	1.326	0.098
HPAIVITGPH	7	0.814	0.048
HPKIVITGPH	8	0.232	0.063
HPSIVITGPH	9	1.043	0.089
HPVIAVTGPS	10	178.002	46.916
HPVIAVTGPX	11	5.733	0.422
HPVIVITGPH	12	1.396	0.128
SCRAMBLED	13	504.810	199.494
HPVIVVTGPH	14	0.745	0.064
HPVIVINGPH	15	28.334	2.744
HPVIAVTGPH	16	280.329	68.591
HAVIVITGPH	17	1.123	0.106
HPAIVITGPH	18	1.133	0.062
HPKIVITGPH	19	0.394	0.120
HPSIVITGPH	20	1.017	0.100
HPVIAVTGPS	21	232.885	47.065
HPVIAVTGPX	22	3.213	0.199
HPVIVITGPH	23	1.481	0.169
SCRAMBLED	24	655.883	352.402
HPVIVVTGPH	25	1.103	0.046
HPVIVINGPH	26	25.669	1.060
HPVIAVTGPH	27	155.776	18.554
HAVIVITGPH	28	1.373	0.073
HPVIAVTGPX	29	3.397	0.154
HPKIVITGPH	30	0.605	0.034
HPSIVITGPH	31	0.586	0.036
HPVIAVTGPS	32	167.046	38.974
HPAIVITGPH	33	0.727	0.053
PALESPRIEITSCLGL	34	35.127	3.567
SPRIEITPSHEL	35	1.988	0.180
ATDTTPSVVVHVCESD	37	400.290	161.175
PIAIIITDTEIS	38	20.728	1.914
PALESPRIEITSCLGL	39	58.305	9.402
SPRIEITPSHEL	40	4.695	1.029
ATDTTPSVVVHVCESD	42	350.579	115.132
PIAIIITDTEIS	43	24.183	2.397
PALESPRIEITSCLGL	44	80.324	15.705
SPRIEITPSHEL	45	1.109	0.071
ATDTTPSVVVHVCESD	47	888.680	817.213
PIAIIITDTEIS	48	18.430	2.877

ASGLLPRIEITPPPEL	48	0.279	0.032	-0.35	0.12

Table S4. List of "calibration" peptides and fit parameters for replicates #1 & #2. Z: phosphothreonine.

Sequence	Code	Calibrated K_d (μM)	Calibrated K_d (μM) Error	PVIVIT ΔΔG (kcal/mol)	PVIVIT ΔΔG (kcal/mol) Error
SCRAMBLED	1	15.245	10.860	2.03	0.71
HPVIVITGPHEE	2	0.500	0.000	0.00	0.00
HPRIVITGPHEE	3	0.486	0.094	-0.02	0.19
HPLIVITGPHEE	4	0.229	0.023	-0.46	0.10
HPVIVIEGPHEE	5	12.022	0.677	1.89	0.06
HPVIVLTGPHEE	6	3.738	0.863	1.19	0.23
IPVIVITGPHEE	7	0.050	0.000	-1.37	0.01
HPVIVITGLHEE	8	5.731	0.293	1.45	0.05
HPVIVITMPHEE	9	1.969	0.181	0.81	0.09
HPKIVITGPHEE	10	0.802	0.164	0.28	0.20
HPKIIITGPHEE	11	0.369	0.089	-0.18	0.24
HPKIVLTGPHEE	12	4.284	0.744	1.27	0.17
HPKIVIQGPHEE	13	9.622	4.827	1.75	0.50
IPKIVITGPHEE	14	0.032	0.002	-1.64	0.06
TPKIVITGPHEE	15	0.159	0.042	-0.68	0.26
HPKIVITTPHEE	16	1.897	0.320	0.79	0.17
HPKIVITNPHEE	17	6.851	1.173	1.55	0.17
HPVIVITGPZEE	22	0.010	0.002	-2.32	0.21
KRMEPIAIIITDTEIS	28	0.654	0.278	0.16	0.43
KRMEPIPIIITDTEIS	29	3.267	0.083	1.11	0.03
KRMEPPAIIITDTEIS	30	0.268	0.138	-0.37	0.52
KRMEPIAIYITDTEIS	31	3.924	0.392	1.22	0.10
KRMEPIAIIITRTEIS	32	1.282	0.690	0.56	0.54
KRMEPIAIIITKTEIS	33	2.227	1.013	0.89	0.45
KRMEPIAIIITDTTIS	34	1.003	0.048	0.41	0.05
ASGLSPRIEITPSHEL	39	12.312	7.502	1.90	0.61
ASGLSPRILITPSHEL	40	0.859	0.132	0.32	0.15
ASGLSPRIAITPSHEL	41	5.065	3.243	1.37	0.64
ASGLSPRIEISPSHEL	42	7.740	0.527	1.62	0.07
ASGLSPRIEIFPSHEL	43	7.595	0.234	1.61	0.03
ASGLLPRIEITPSHEL	44	1.039	0.022	0.43	0.02
ASGLSPRIEITPFHEL	45	3.816	1.291	1.21	0.34
ASGLSPRIEITASHEL	46	5.050	0.182	1.37	0.04

Table S5. List of "full calibration replicate #1 and #2" peptides and fit parameters. Z: phosphothreonine.

Sequence	Code	Calibrated K_d (μM)	Calibrated K_d (μM) Error	PVIVIT ΔΔG (kcal/mol)	PVIVIT ΔΔG (kcal/mol) Error
SCRAMBLED	1	20.937	16.943	2.21	0.81
HPVIVITGPHEE	2	0.500	0.000	0.00	0.00
HPRIVITGPHEE	3	0.535	0.152	0.04	0.28
HPLIVITGPHEE	4	0.267	0.018	-0.37	0.07
HPVIVIEGPHEE	5	10.660	2.117	1.81	0.20
HPVIVLTGPHEE	6	3.019	0.920	1.07	0.30
IPVIVITGPHEE	7	0.075	0.006	-1.12	0.09
HPVIVITGLHEE	8	3.165	0.488	1.09	0.15
HPVIVITMPHEE	9	1.696	0.195	0.72	0.11
HPKIVITGPHEE	10	0.901	0.208	0.35	0.23
HPKIIITGPHEE	11	0.349	0.005	-0.21	0.01
HPKIVLTGPHEE	12	4.066	0.831	1.24	0.20
IPKIVITGPHEE	14	0.056	0.007	-1.29	0.12
TPKIVITGPHEE	15	0.157	0.003	-0.69	0.02
HPKIVITTPHEE	16	1.738	0.392	0.74	0.23
HPKIVITNPHEE	17	6.057	1.883	1.48	0.31
IPKIIITYPGEE	18	0.500	0.154	0.00	0.31
VPKIIITYPGEE	19	0.403	0.127	-0.13	0.31
IPKIIVTYPGEE	20	0.266	0.065	-0.38	0.24
IPKIIVTYPDEE	21	0.315	0.022	-0.27	0.07
HPVIVITGPZEE	22	0.019	0.002	-1.95	0.09
IPKIIVTAPZEE	24	0.004	0.001	-2.80	0.18
VPRIIITKPZEE	25	0.003	0.001	-2.99	0.24
IPKIIITYPZEE	27	0.011	0.004	-2.27	0.38
KRMEPIAIIITDTEIS	28	0.599	0.242	0.11	0.40
KRMEPIPIIITDTEIS	29	4.473	0.103	1.30	0.02
KRMEPPAIIITDTEIS	30	0.342	0.140	-0.22	0.41
KRMEPIAIYITDTEIS	31	3.161	0.804	1.09	0.25
KRMEPIAIIITRTEIS	32	0.449	0.283	-0.06	0.63
KRMEPIAIIITKTEIS	33	0.943	0.449	0.38	0.48
KRMEPIAIIITDTTIS	34	0.723	0.011	0.22	0.02
KRMEPPKIIITDTEIS	36	0.083	0.041	-1.06	0.49
KRMEPPKIIITDTSIS	37	0.108	0.014	-0.91	0.12
ASGLLPRIIITPPYEL	38	0.025	0.005	-1.77	0.19
ASGLSPRIEITPSHEL	39	10.671	5.536	1.81	0.52
ASGLSPRILITPSHEL	40	0.672	0.185	0.18	0.27
ASGLSPRIAITPSHEL	41	4.993	3.301	1.36	0.66
ASGLSPRIEISPSHEL	42	7.109	0.483	1.57	0.07
ASGLSPRIEIFPSHEL	43	5.280	1.029	1.40	0.19
ASGLLPRIEITPSHEL	44	1.107	0.003	0.47	0.00
ASGLSPRIEITPFHEL	45	3.855	0.855	1.21	0.22
ASGLSPRIEITASHEL	46	4.347	0.184	1.28	0.04

Table S6. Calculated savings and references vs other techniques.

Methods	Number of peptides	Amount of Protein (µg)[e]	X Time MRBLE
MRBLE	1	32	1
MRBLE	96	32	1
MRBLE	384	32	1
FP[a]	1	60	1.875
FP[a]	96	5760	180
FP[a]	384	23040	720
SPR[b]	1	40	1.25
SPR[b]	96	3840	120
SPR[b]	384	15360	480
GST[c]	1	20	0.625
GST[c]	96	1920	60
GST[c]	384	7680	240
ITC[d]	1	800	25
ITC[d]	96	76800	2400
ITC[d]	384	307200	9600

Notes: a. Fluorescence polarization[7,8], b. surface plasmon resonance[9], c. glutathione S-transferase pull-down[10,11] d. isothermal titration calorimetry[12], e. amount of protein estimated from published available protocols.

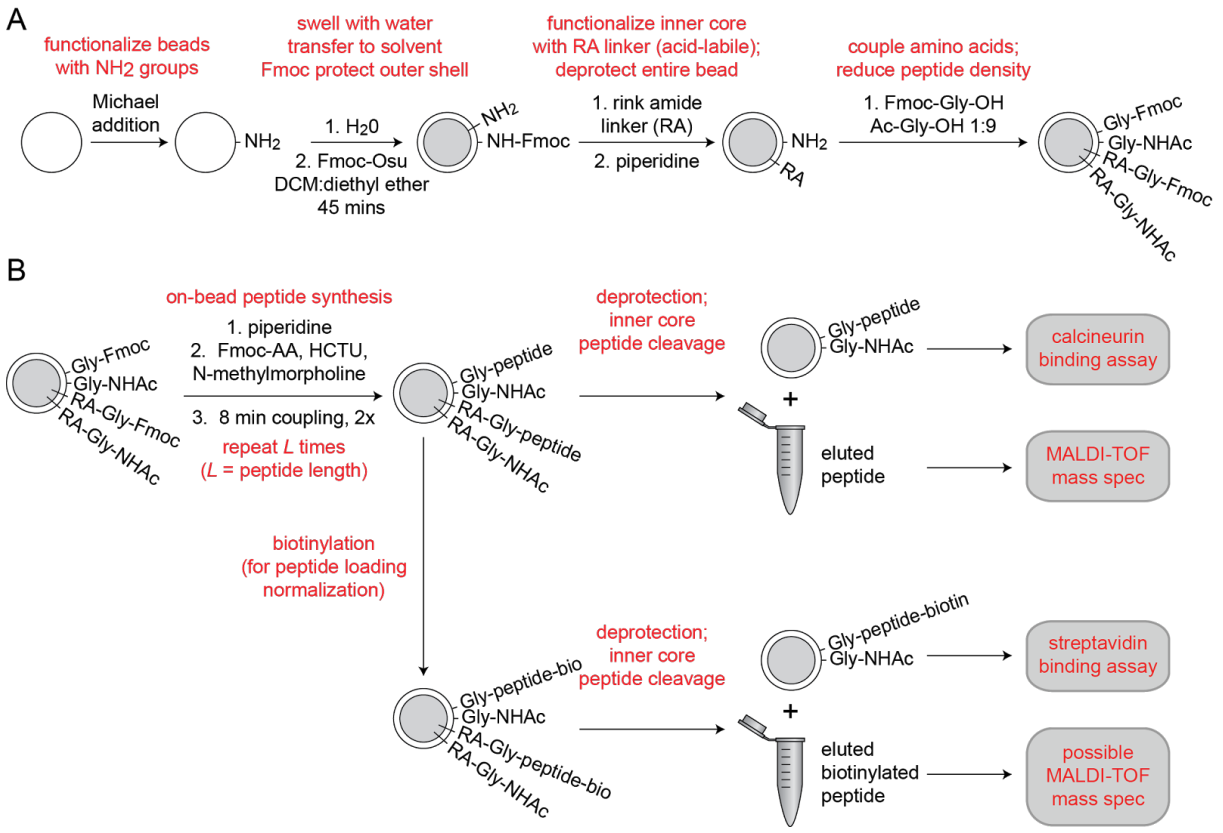

Figure S1. Integrated peptide quality control and quantification. **(A)** Synthesis scheme for functionalizing MRBLE cores with an acid-labile rink amide linker and MRBLE shells with an acid-resistant glycine linker[13]. **(B)** Experimental pipeline for peptide elution, quality control, and quantification.

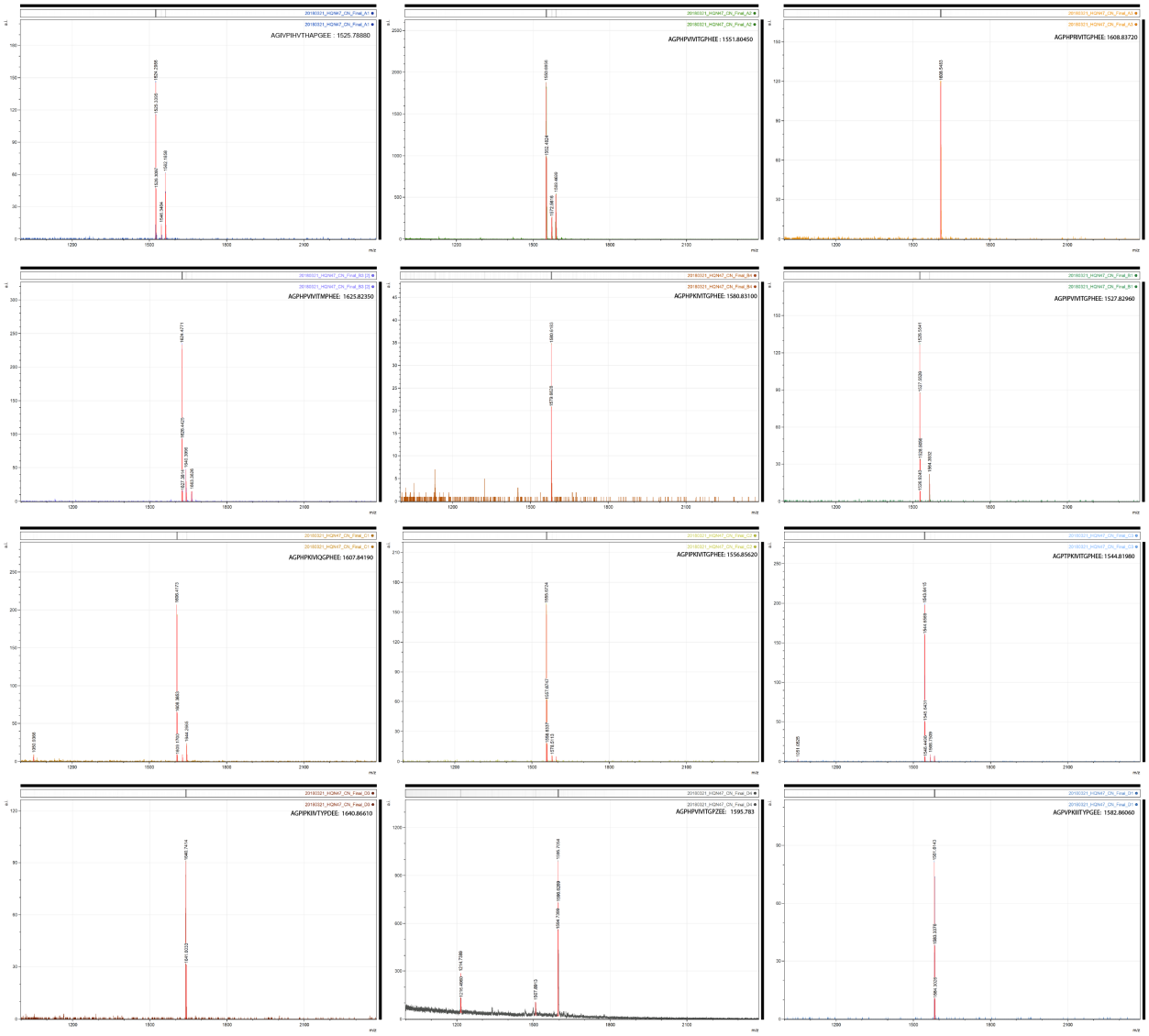

Figure S2a. Mass spectrometry data of full calibration peptides. MALDI-TOF traces for all 48 peptides obtained using Bruker microflex MALDI-TOF (Billerica, MA, USA). The instrument was run on positive-ion reflector mode with a laser setting of 1,810 V and data averaged over 100 scans. Raw data was analyzed using FlexAnalysis and mMass (ver. 5.5, www.mmass.org). Z: phosphothreonine.

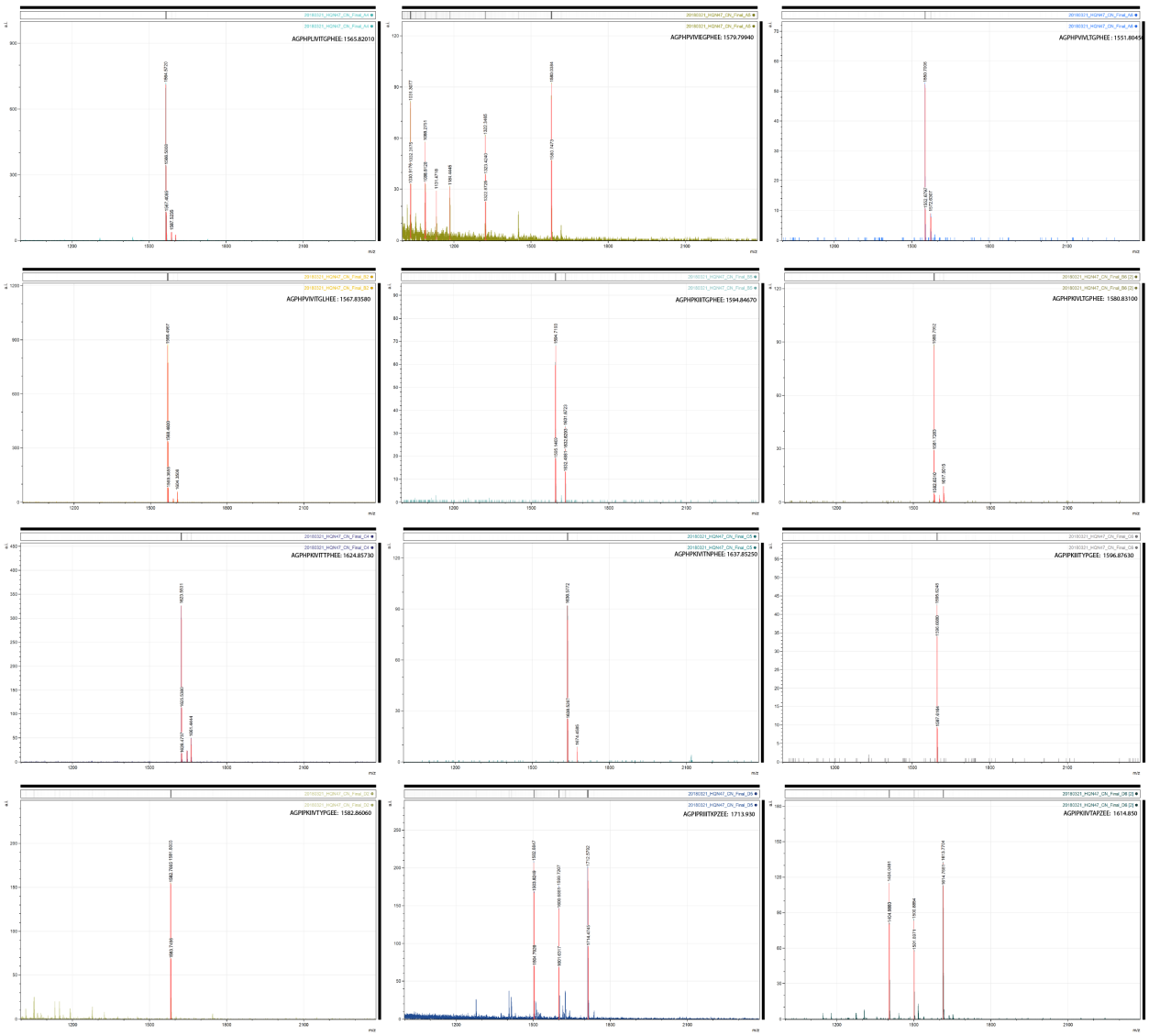

Figure S2b. Mass spectrometry data of full calibration peptides. MALDI-TOF traces for all 48 peptides obtained using Bruker microflex MALDI-TOF (Billerica, MA, USA). The instrument was run on positive-ion reflector mode with a laser setting of 1,810 V and data averaged over 100 scans. Raw data was analyzed using FlexAnalysis and mMass (ver. 5.5, www.mmass.org). Z: phosphothreonine. Loss of an E and hydrolysis of phosphate was observed for phosphopeptides.

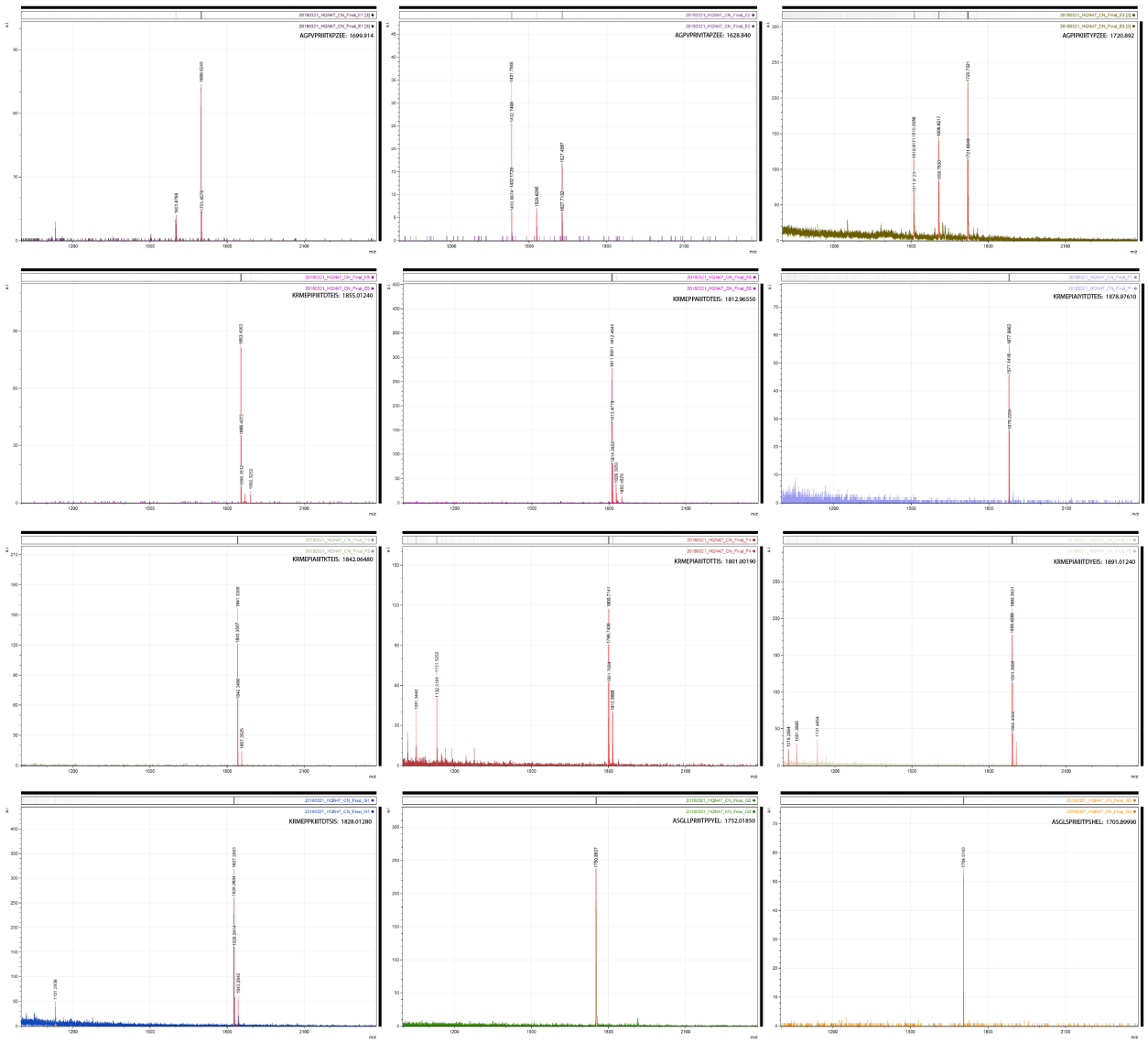

Figure S2c. Mass spectrometry data of full calibration peptides. MALDI-TOF traces for all 48 peptides obtained using Bruker microflex MALDI-TOF (Billerica, MA, USA). The instrument was run on positive-ion reflector mode with a laser setting of 1,810 V and data averaged over 100 scans. Raw data was analyzed using FlexAnalysis and mMass (ver. 5.5, www.mmass.org). Z: phosphothreonine. Loss of an E and hydrolysis of phosphate was observed for phosphopeptides.

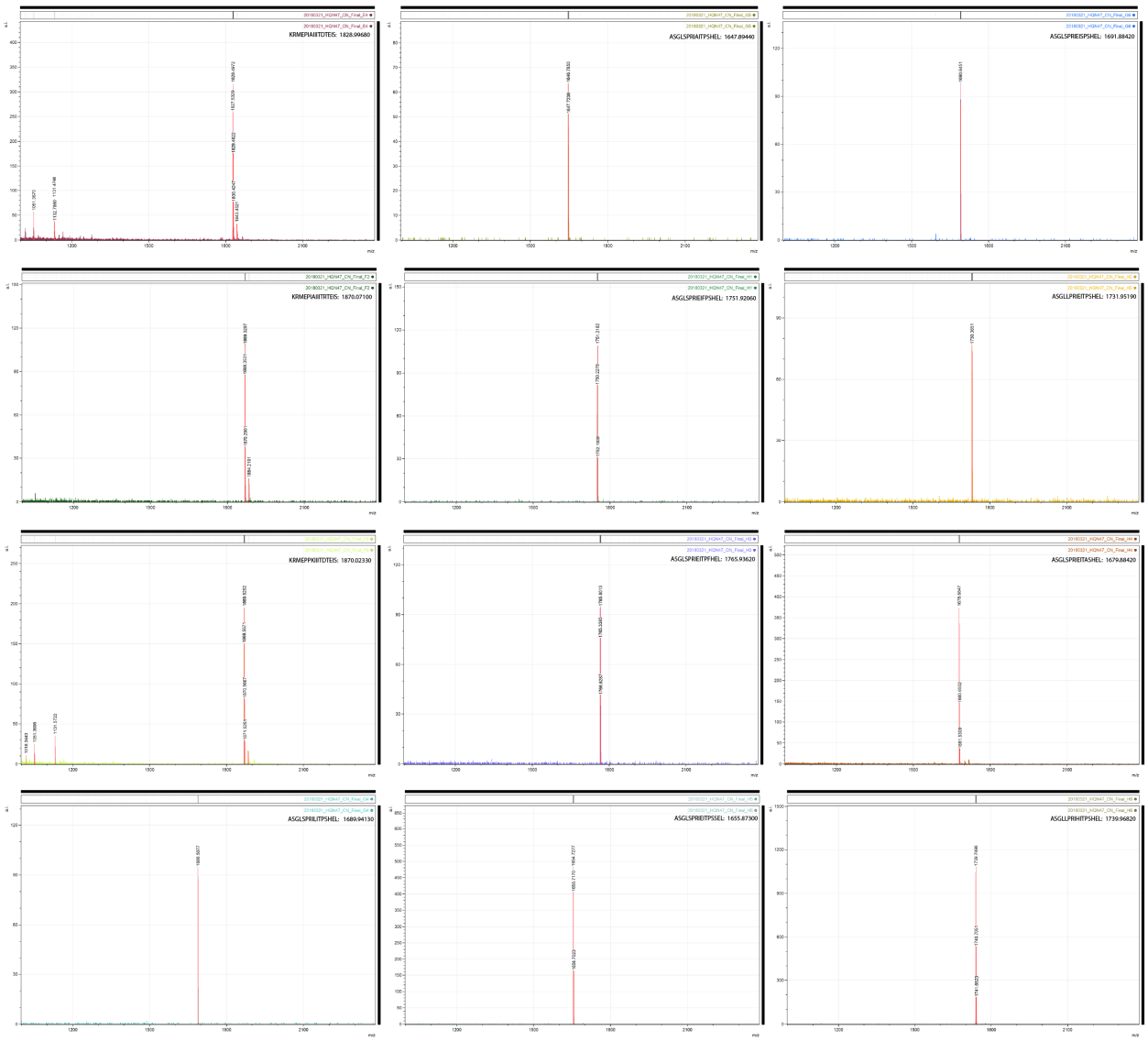

Figure S2d. Mass spectrometry data of full calibration peptides. MALDI-TOF traces for all 48 peptides obtained using Bruker microflex MALDI-TOF (Billerica, MA, USA). The instrument was run on positive-ion reflector mode with a laser setting of 1,810 V and data averaged over 100 scans. Raw data was analyzed using FlexAnalysis and mMass (ver. 5.5, www.mmass.org). Z: phosphothreonine.

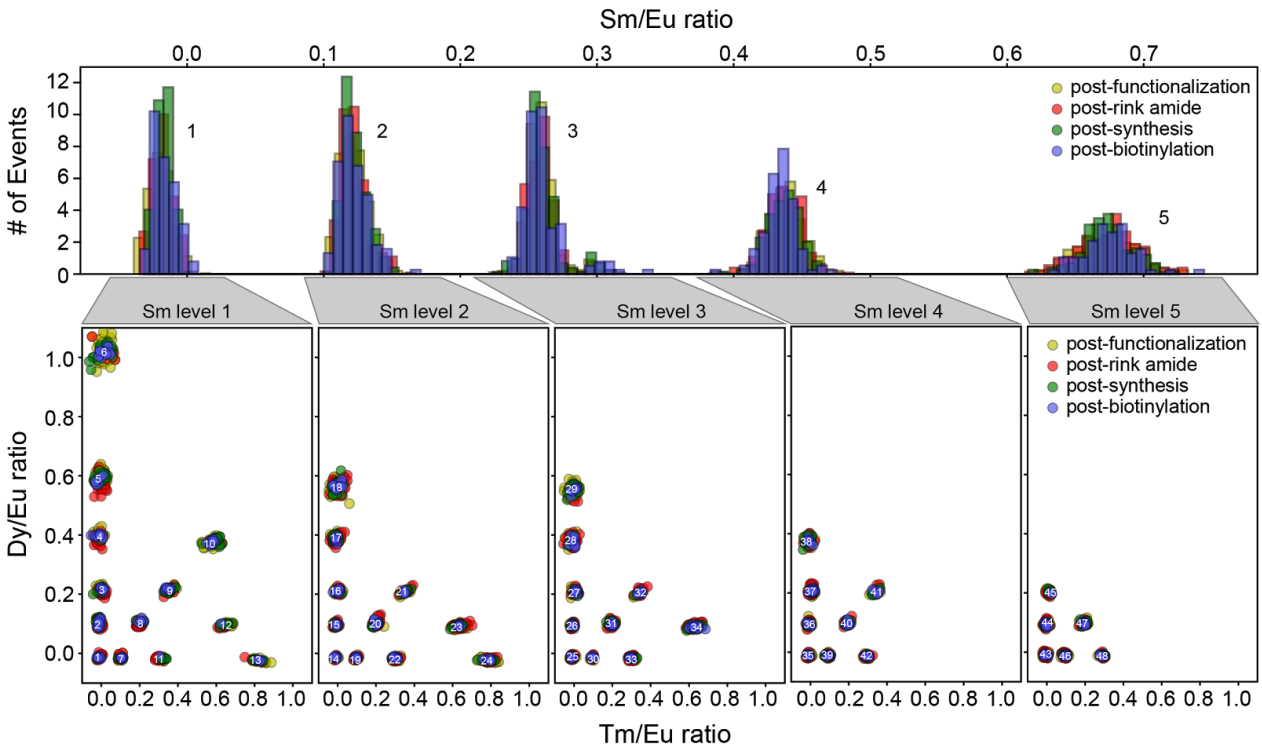

Figure S3. MRBLE spectral codes are unaffected by chemical reagents required for peptide synthesis. Each embedded MRBLE code is composed of a unique combination of 4 lanthanides (Europium (Eu), Dysprosium (Dy), Samarium (Sm), and Thulium (Tm)) and expressed in terms of 3 ratios (Sm/Eu, Dy/Eu, and Tm/Eu). Histograms of Sm/Eu ratios within each bead remain unchanged after bead functionalization, rink amide coupling, peptide synthesis, and biotinylation (top). Scatter plots of Dy/Eu and Tm/Eu ratios for each of 5 possible Sm/Eu ratios demonstrate that these ratios also remain constant throughout the synthesis process (bottom).

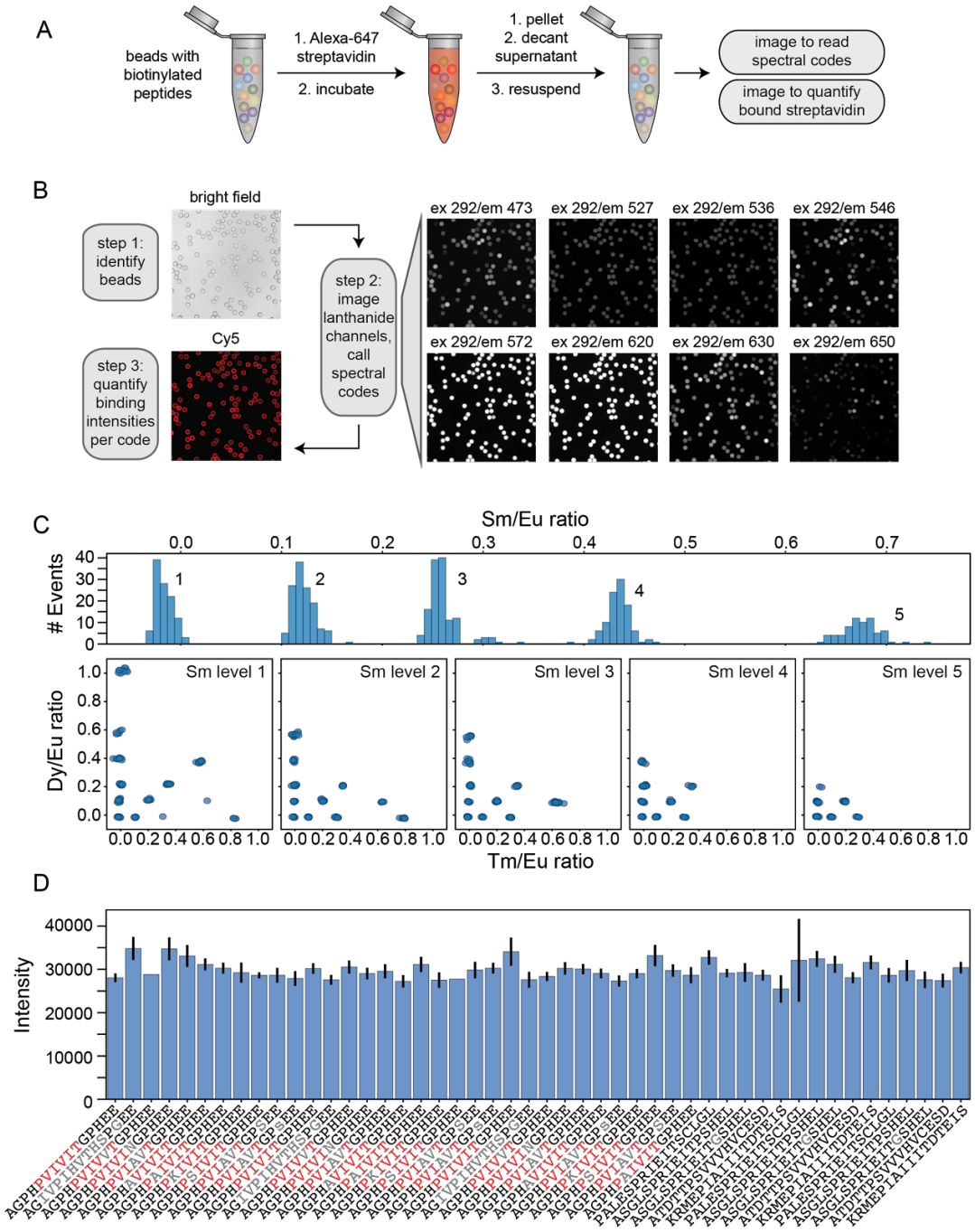

Figure S4. Streptavidin binding assay reveals any sequence-specific differences in peptide synthesis efficiency. **(A)** Experimental pipeline for streptavidin binding assay. MRBLE peptide libraries are biotinylated, incubated with Alexa-647-labeled streptavidin, washed, and imaged to identify embedded spectral codes and peptide sequences associated with each bead as well as quantify the amount of bound streptavidin. **(B)** Example images showing Alexa-647-labeled streptavidin binding to biotinylated MRBLE libraries and image processing steps. **(C)** Histograms and scatter plots of MRBLE Sm/Eu, Dy/Eu, and Tm/Eu ratios showing 48 clearly resolved intensity clusters and resolvable spectral codes. **(D)** Measured bound streptavidin intensities (median +/- standard error on the mean) for an example 48-code library containing multiple systematic variants of candidate calcineurin substrates.

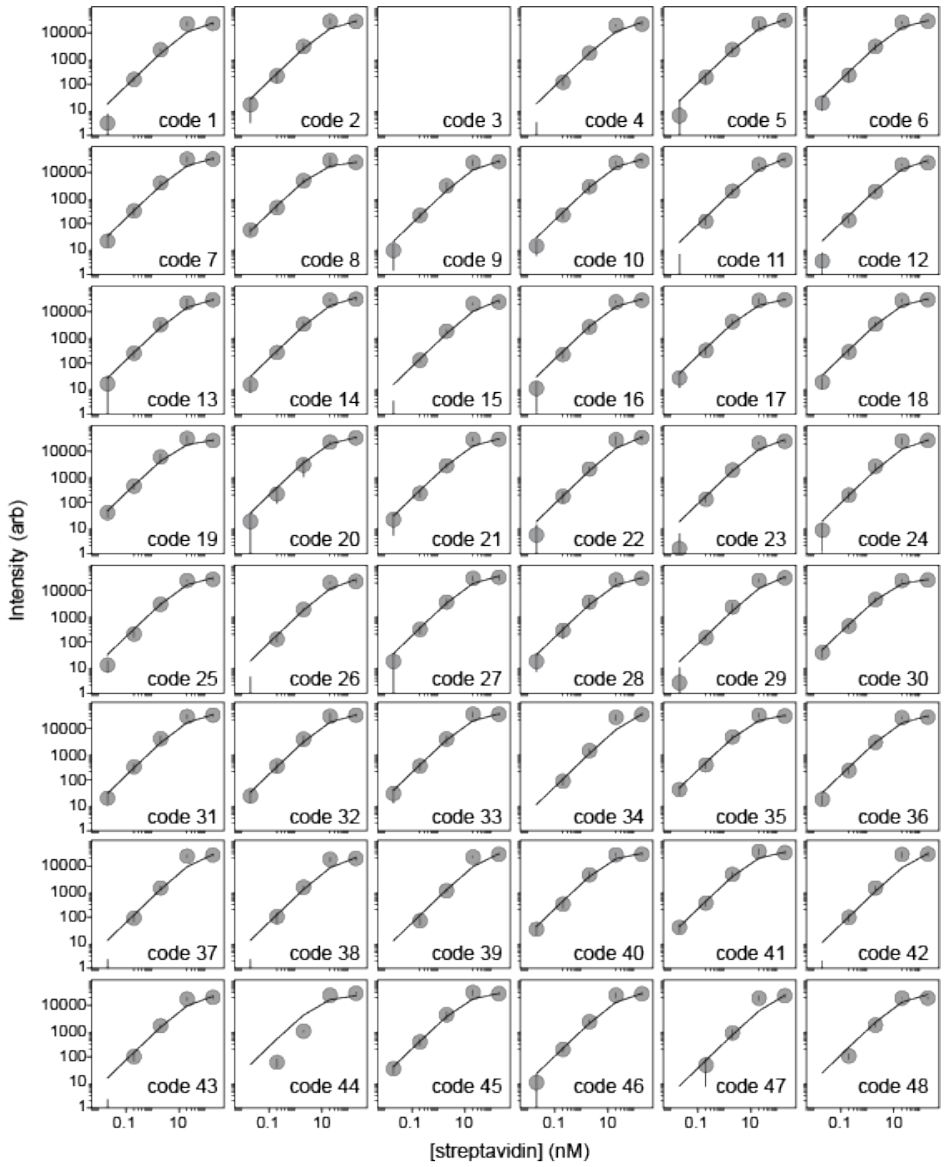

Figure S5. Streptavidin binding assay can be used to determine peptide loading density. Scatter plots of measured intensity per bead (median +/- s.e.m) as a function of Alexa-647-labeled streptavidin concentration demonstrate that intensities saturate at approximately 20 nM labeled streptavidin. Each reaction includes ~ 7000 total beads in a 100 µL volume, suggesting that each individual bead displays ~ 2 x 10^8 peptides.

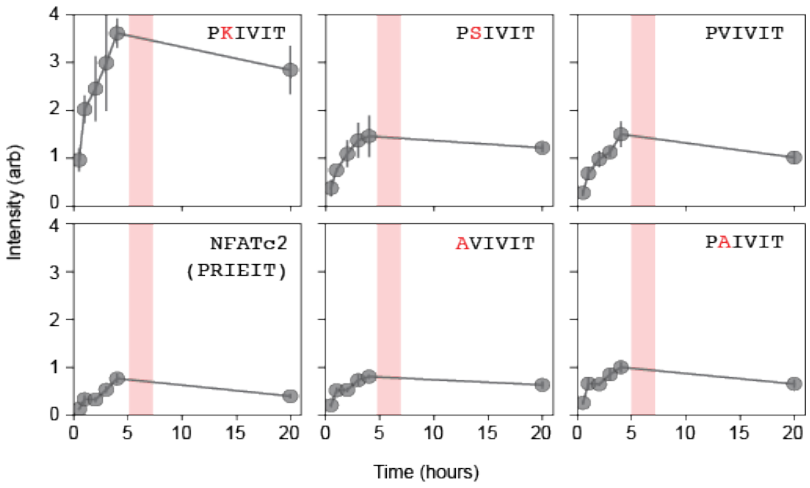

Figure S6. Time-dependent measurements of calcineurin binding demonstrating that calcineurin-MRBLE on-rates are slow and reach equiluibrium only after ~ 5-6 hours. Measured intensities (grey dots with interpolated line) for 6 PxIxIT variant peptides (PKIVIT, PSIVIT, PVIVIT, NFATc2, AVIVIT, and PAIVIT) as a function of time for a reaction concentration of 0.25 µM calcineurin. Intensities appear to saturate at ~ 5-6 hours and decrease only slightly after 24 hours. Pink boxes signify the time window for all subsequent measurements.

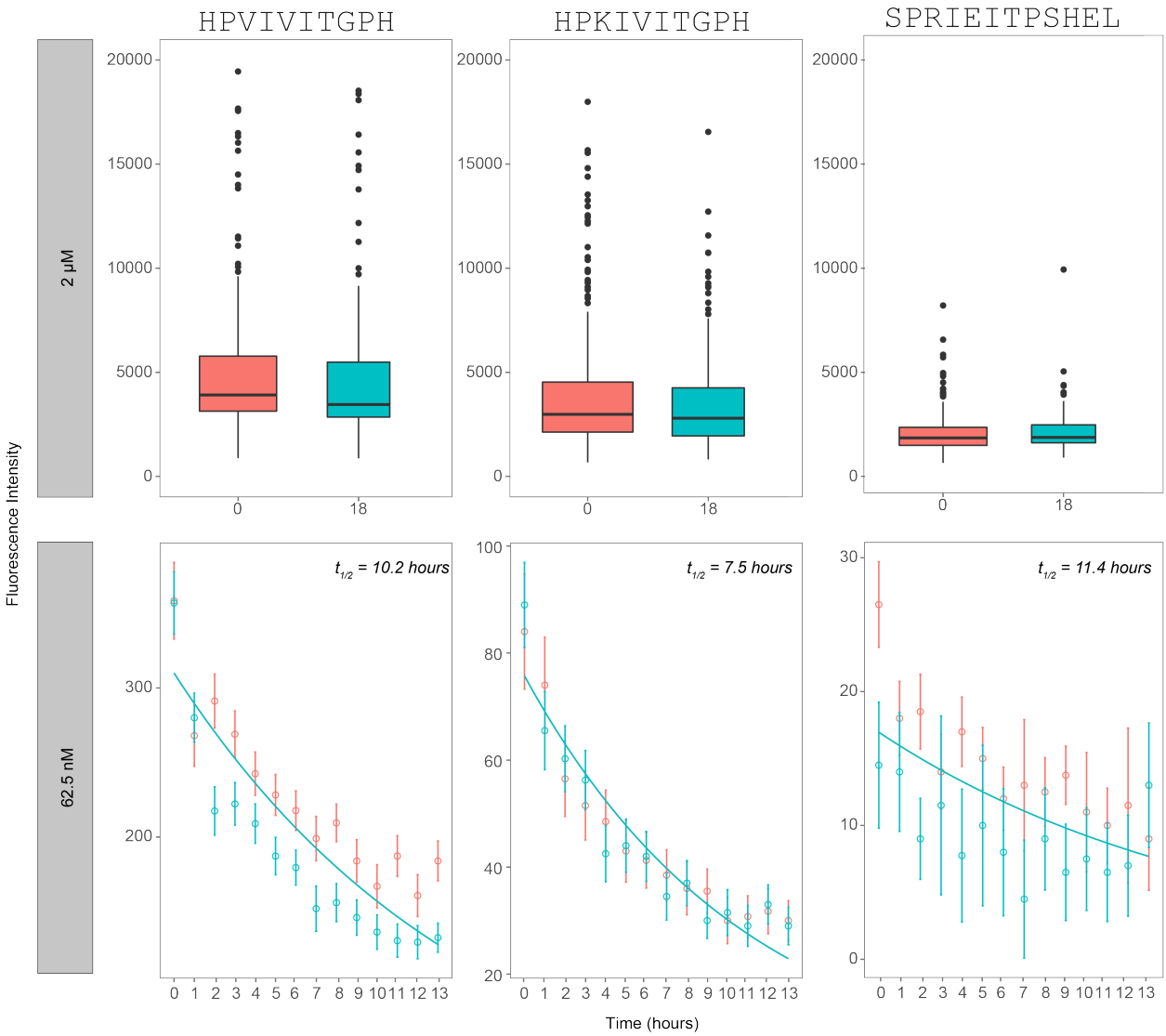

Figure S7. Dissociation rate of calcineurin over a time period of ~13-18 hours after reaching equilibrium. Measured intensities for 3 PxIxIT variant peptides (PKIVIT, PVIVIT, and NFATc2) as a function of time for a reaction concentration of 2 µM calcineurin (top panel) and 62.5 nM (bottom panel). Bottom panel represent replicates of the same peptide sequences on 2 separate codes and are indicated by different colors (blue/red).

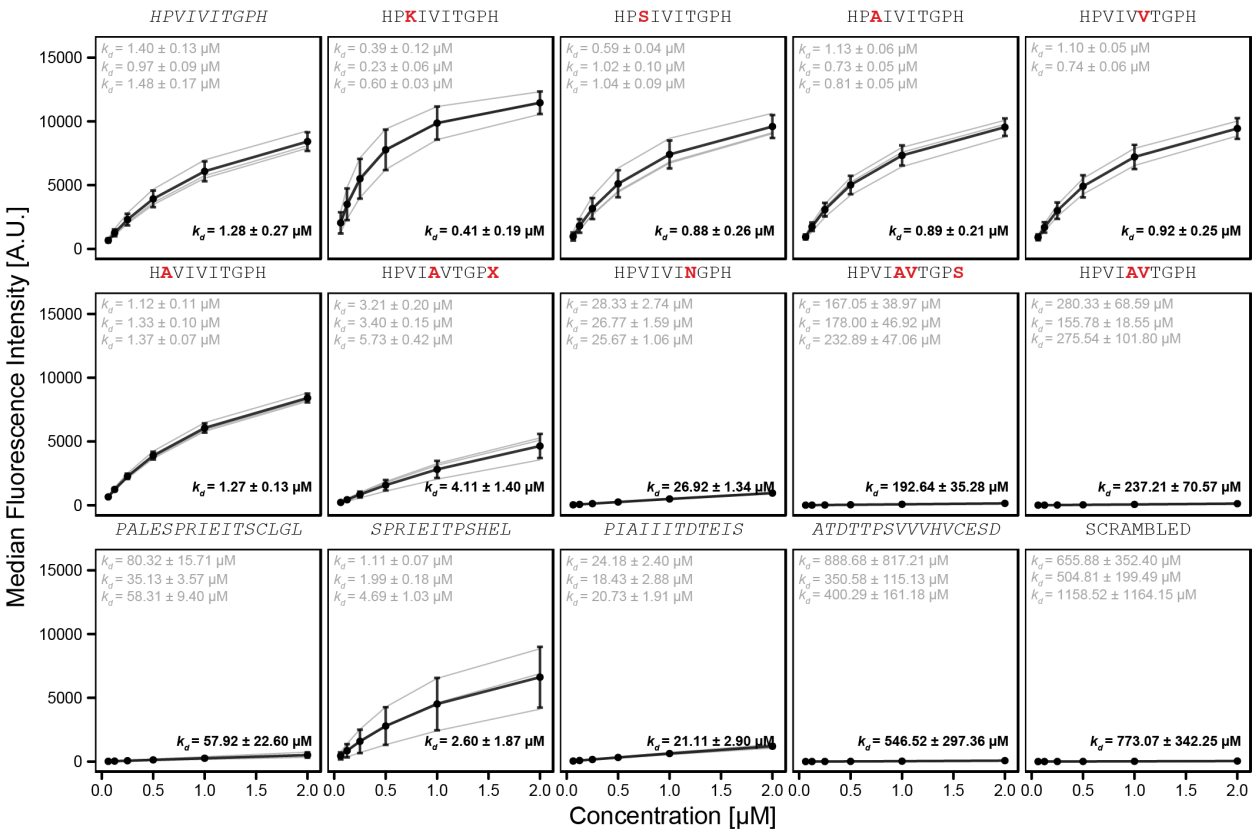

Figure S8. Triplicate library of reported PVIVIT and natural variants. Amino acid letter in red text indicate the mutation from WT sequence (grey). Each peptide was synthesized separately onto 3 different codes (with the exception of HPVIVVTGPH with only 2 codes). Binding curves were fit with a Langmuir isotherm model to estimate binding affinity (K_d).

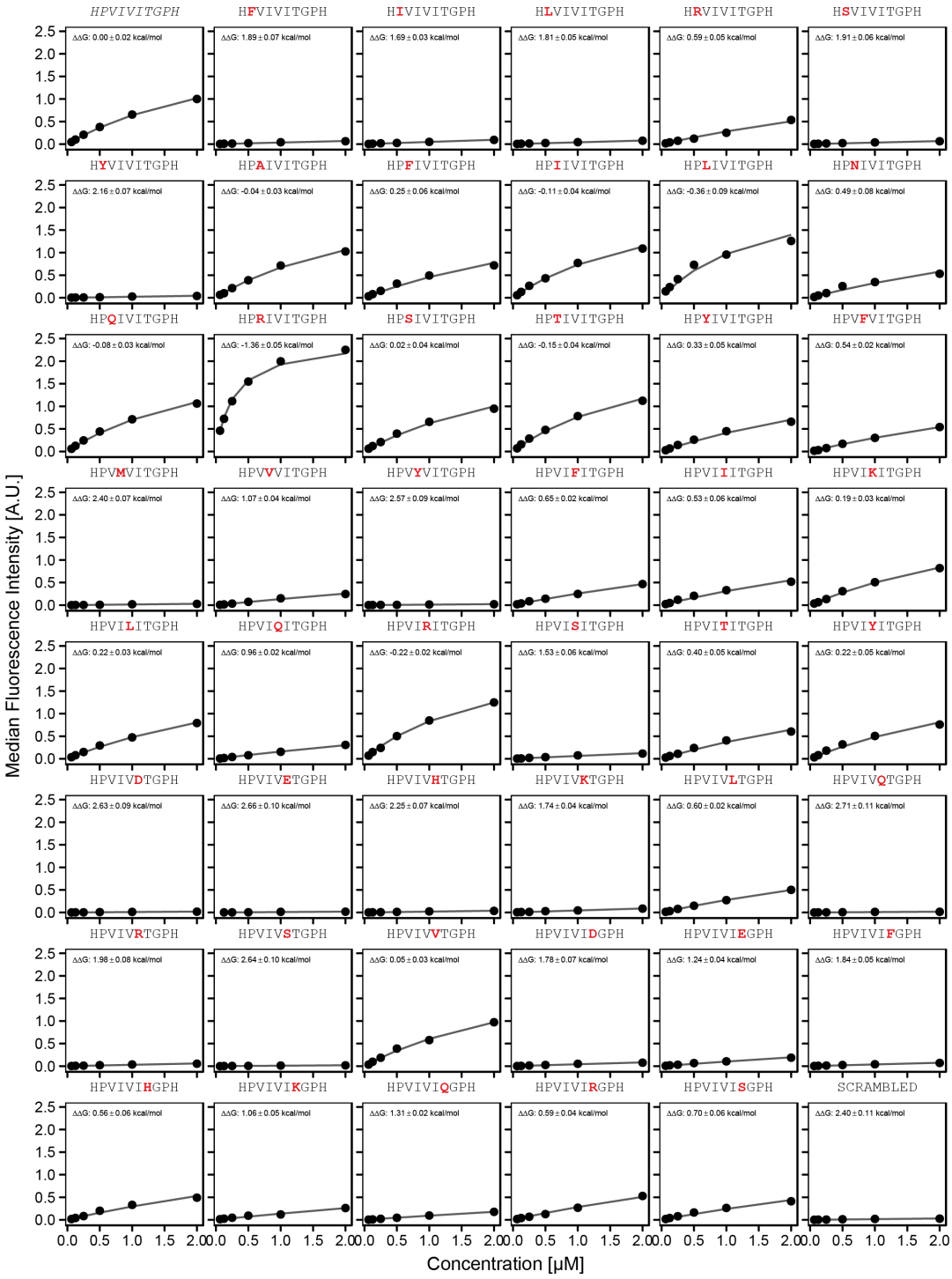

Figure S9. PVIVIT core mutation library. Concentration-dependent binding measurements for systematic mutations within the PVIVIT core motif. For each sequence, measured change in binding affinity relative to the wild-type PVIVIT sequence was determined by a global fit to a single-site binding model (black line). The wild-type sequence is shown in italics and single amino acid substitutions are shown in red.

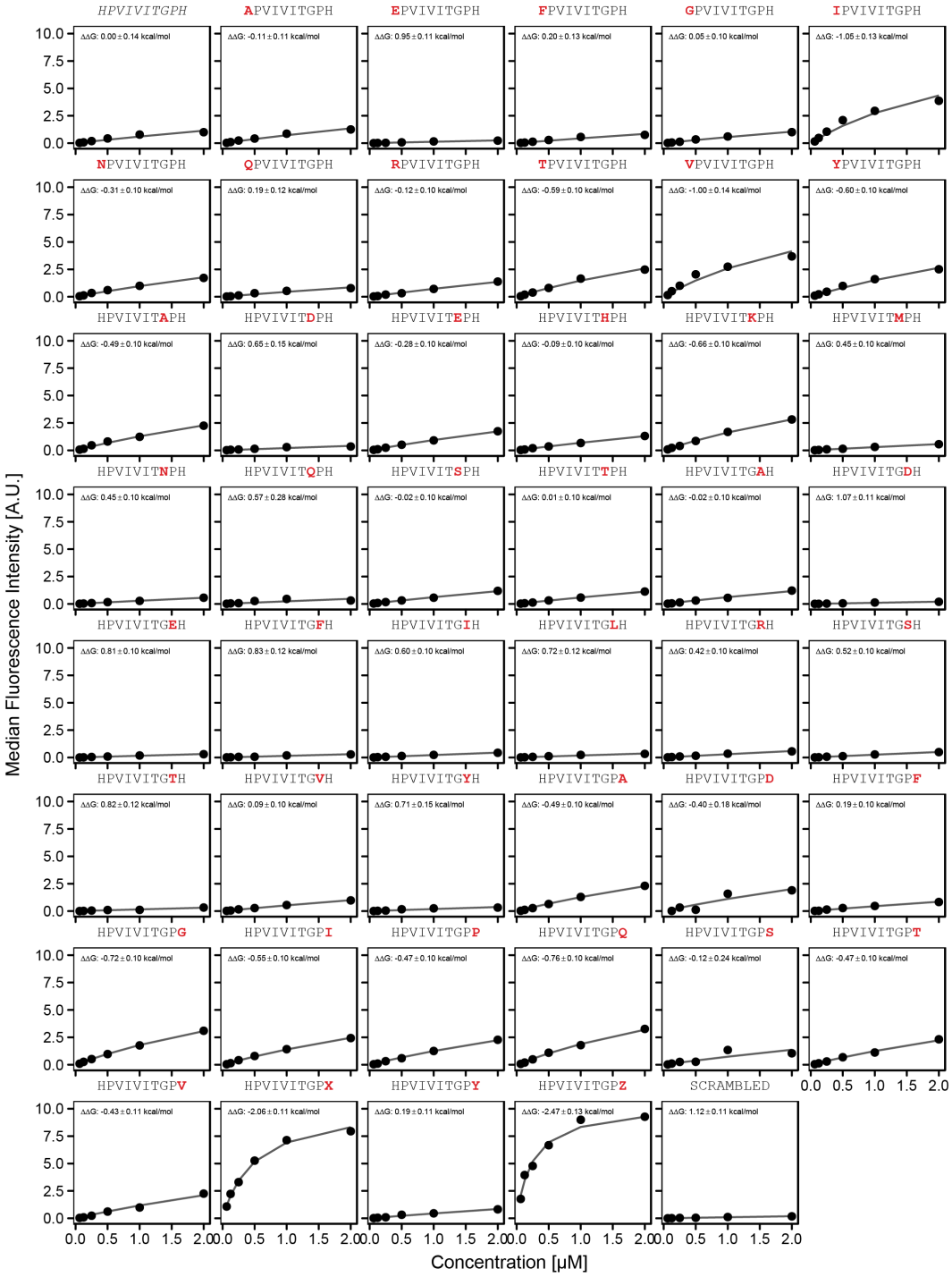

Figure S10. PVIVIT flank mutation library. Concentration-dependent binding measurements for systematic mutations flanking the PVIVIT core motif. For each sequence, measured change in binding affinity relative to the wild-type PVIVIT sequence was determined by a global fit to a single-site binding model (black line). The wild-type sequence is shown in italics and single amino acid substitutions are shown in red.

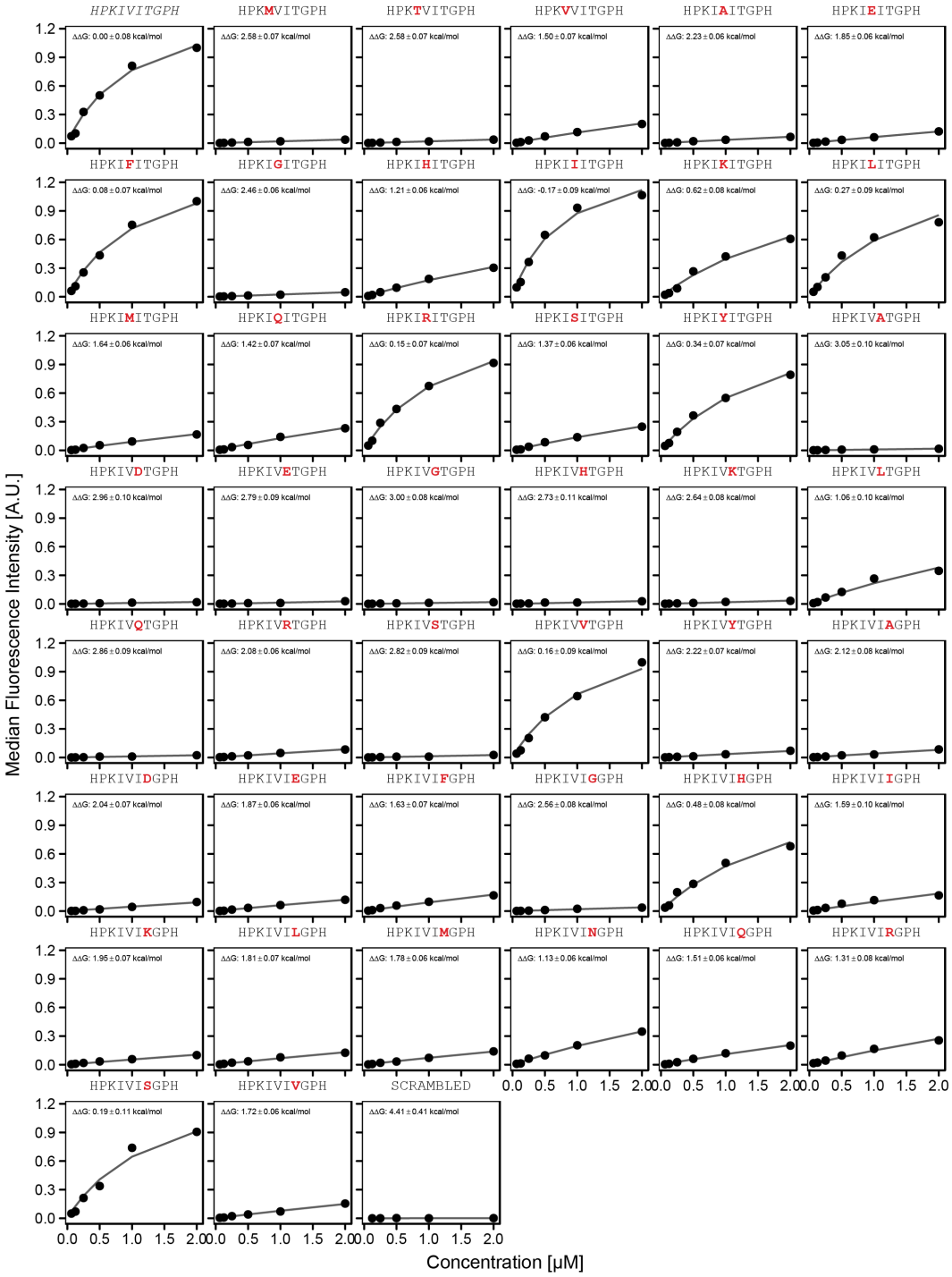

Figure S11. PKIVIT core mutation library. Concentration-dependent binding measurements for systematic mutations within the PKIVIT core motif. For each sequence, measured change in binding affinity relative to the wild-type PKIVIT sequence was determined by a global fit to a single-site binding model (black line). The wild-type sequence is shown in italics and single amino acid substitutions are shown in red.

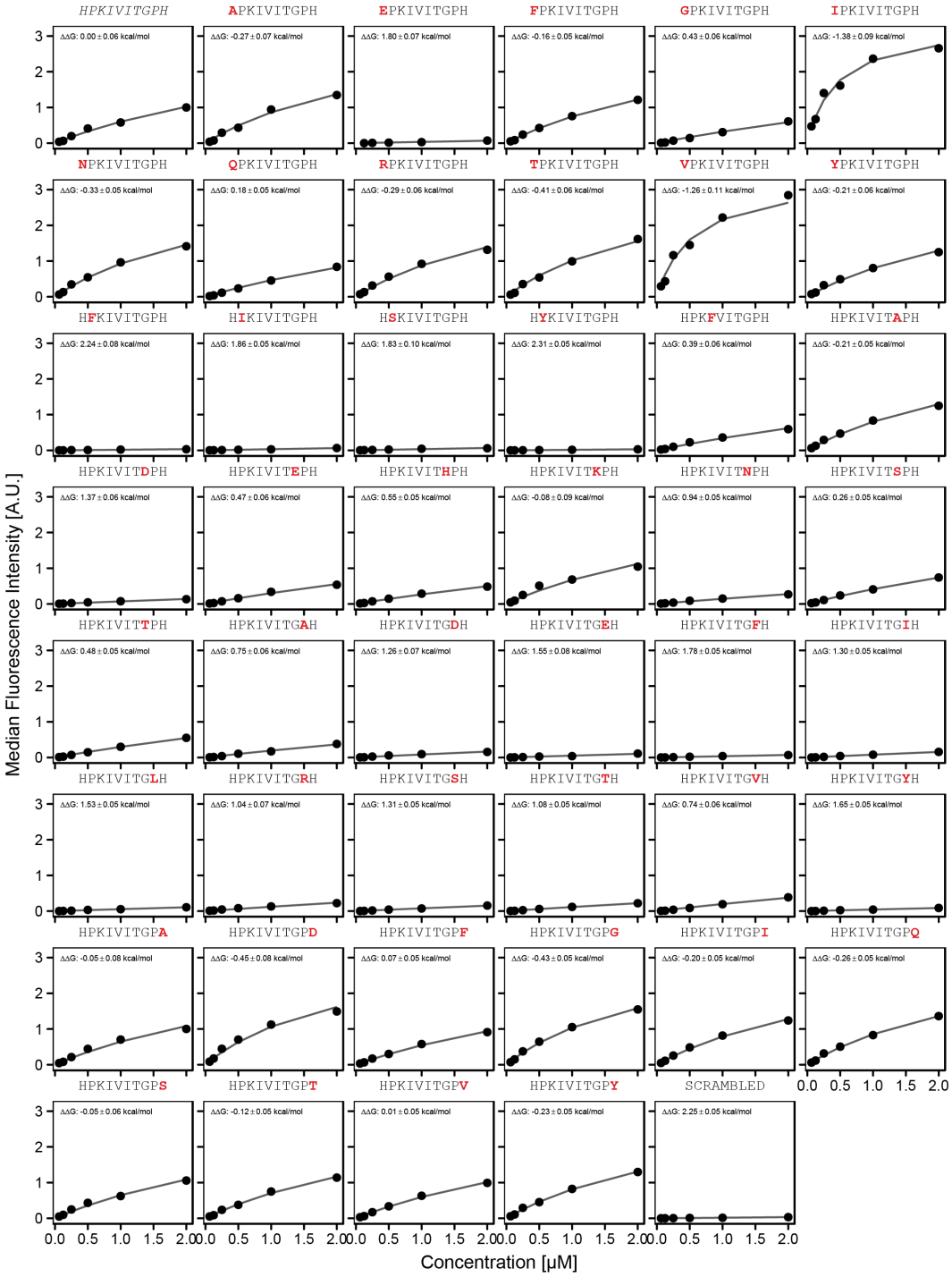

Figure S12. PKIVIT flank mutation library. Concentration-dependent binding measurements for systematic mutations flanking the PKIVIT core motif. For each sequence, measured change in binding affinity relative to the wild-type PKIVIT sequence was determined by a global fit to a single-site binding model (black line). The wild-type sequence is shown in italics and single amino acid substitutions are shown in red.

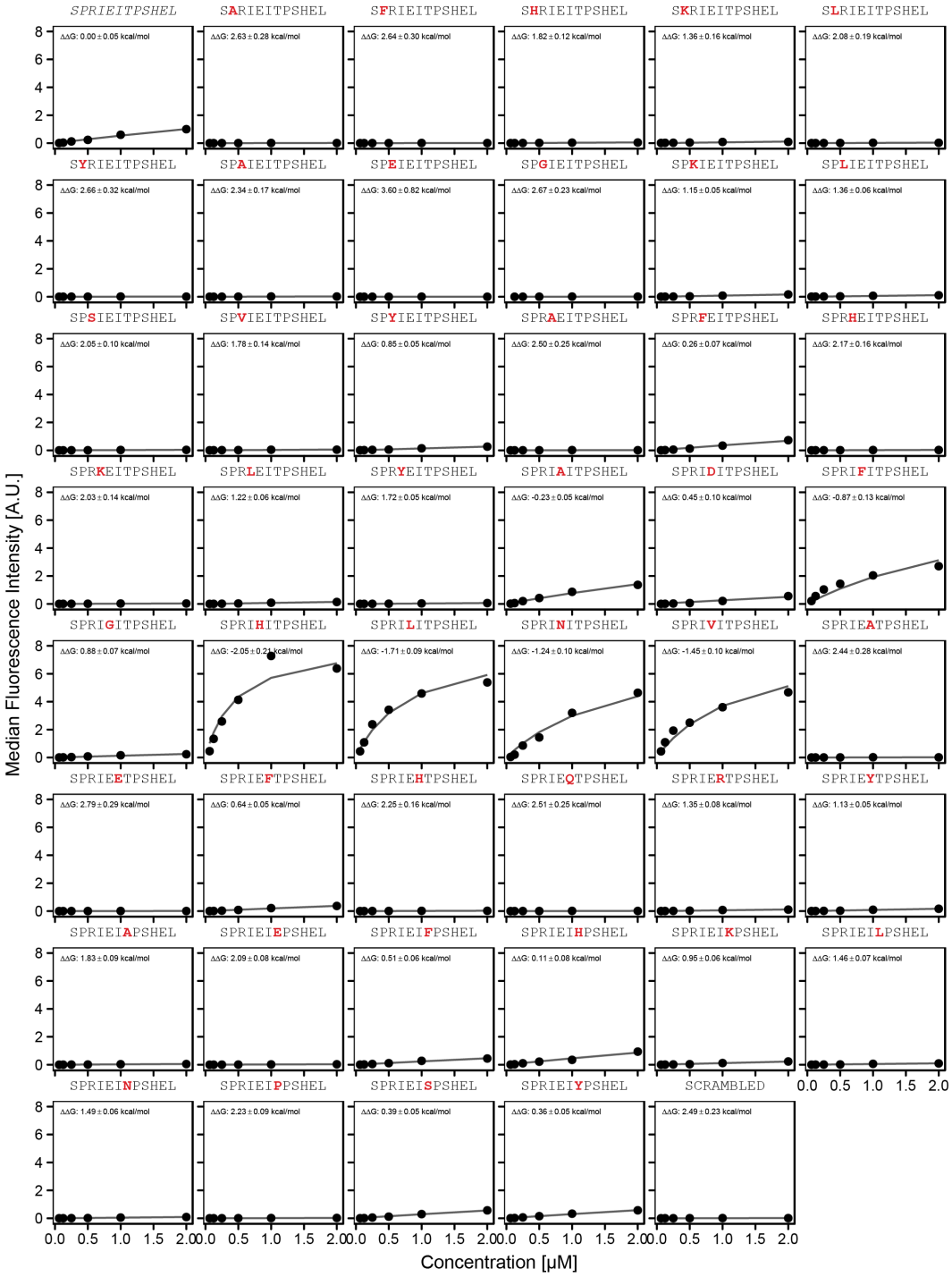

Figure S13. NFATc2 (PRIEIT) core mutation library. Concentration-dependent binding measurements for systematic mutations within the NFATc2 core motif. For each sequence, measured change in binding affinity relative to the wild-type PRIEIT sequence was determined by a global fit to a single-site binding model (black line). The wild-type sequence is shown in italics and single amino acid substitutions are shown in red.

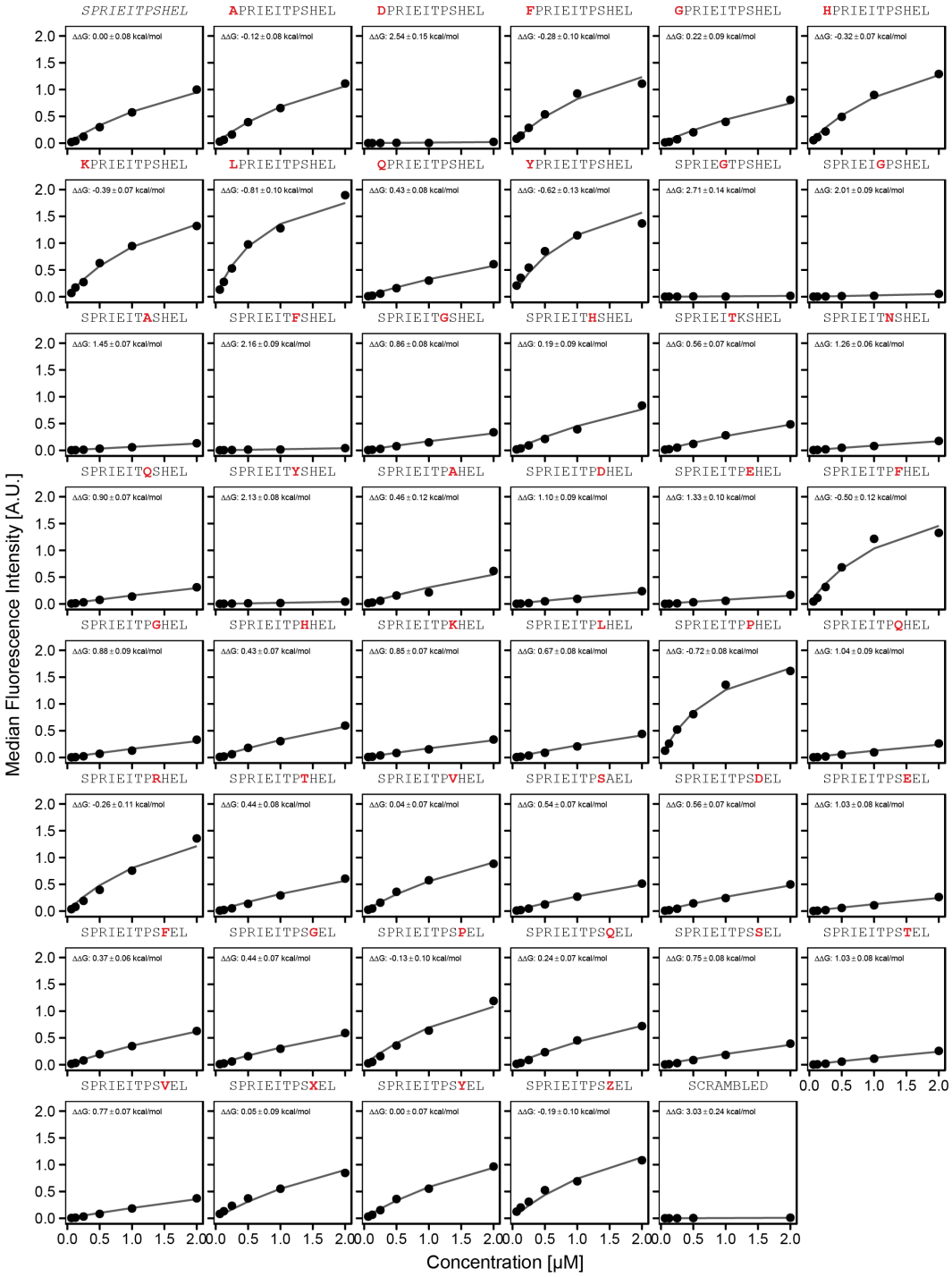

Figure S14. NFATc2 (PRIEIT) flank mutation library. Concentration-dependent binding measurements for systematic mutations flanking the NFATc2 core motif. For each sequence, measured change in binding affinity relative to the wild-type PRIEIT sequence was determined by a global fit to a single-site binding model (black line). The wild-type sequence is shown in italics and single amino acid substitutions are shown in red.

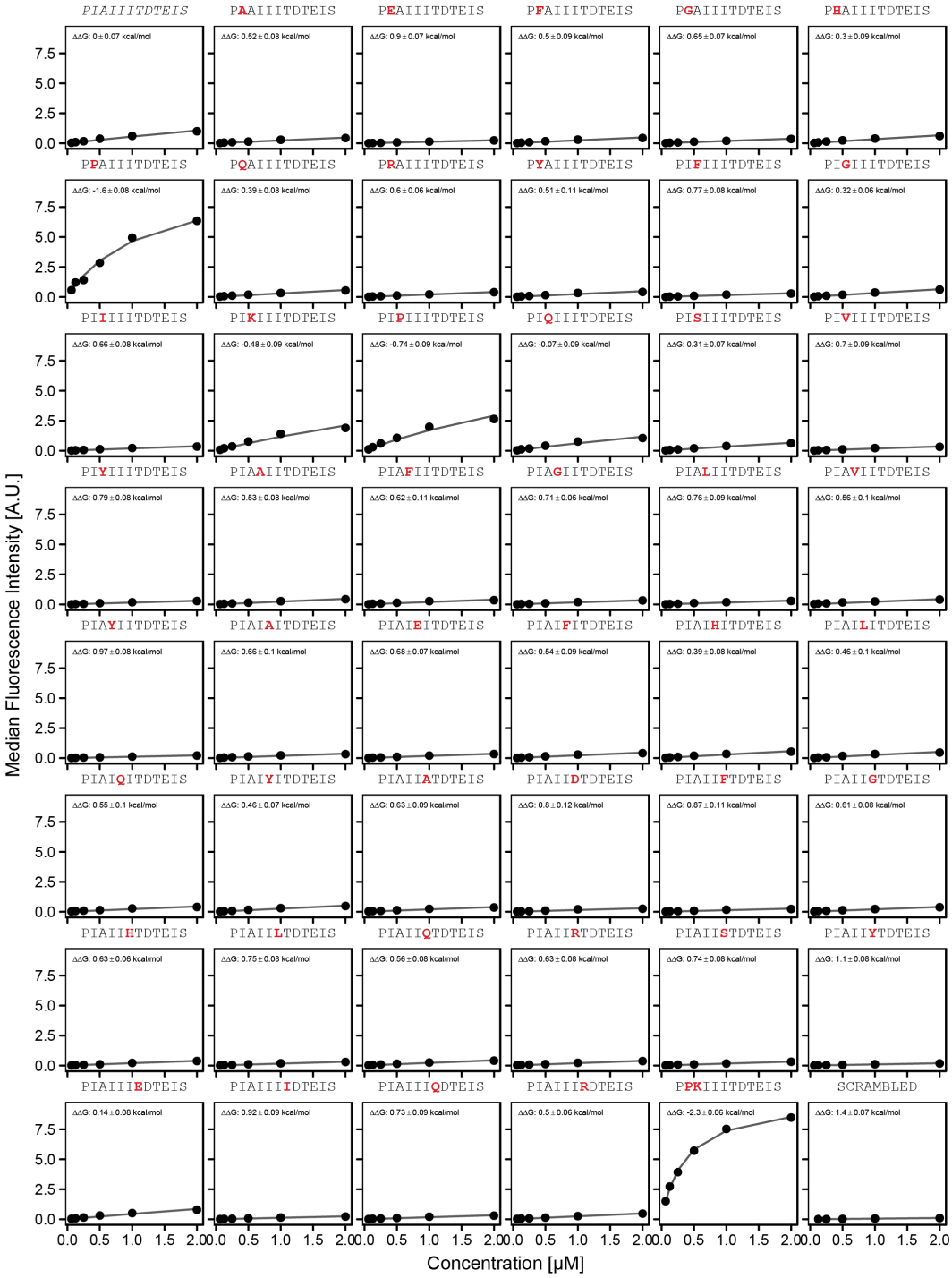

Figure S15. AKAP79 (IAIIIT) core mutation library. Concentration-dependent binding measurements for systematic mutations within the NFATc2 core motif. For each sequence, measured change in binding affinity relative to the wild-type IAIIIT sequence was determined by a global fit to a single-site binding model (black line). The wild-type sequence is shown in italics and single amino acid substitutions are shown in red.

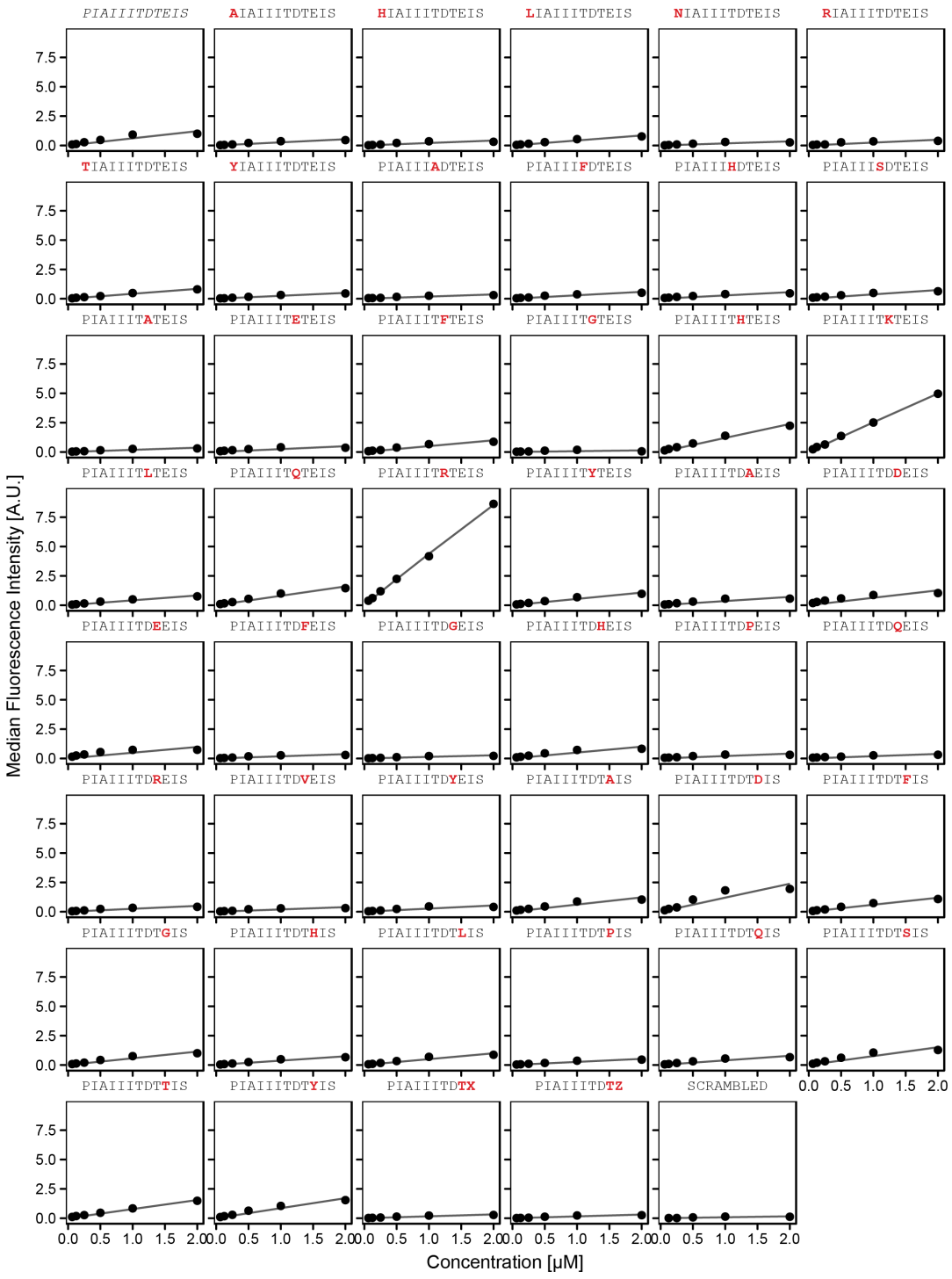

Figure S16. AKAP79 (IAIIIT) flanking mutation library. Concentration-dependent binding measurements for systematic mutations flanking the AKAP79 core motif. For each sequence, measured change in binding affinity relative to the wild-type PRIEIT sequence was determined by a global fit to a single-site binding model (black line); however, a lack of saturation precluded quantitative determination of changes in affinity. The wild-type sequence is shown in italics and single amino acid substitutions are shown in red.

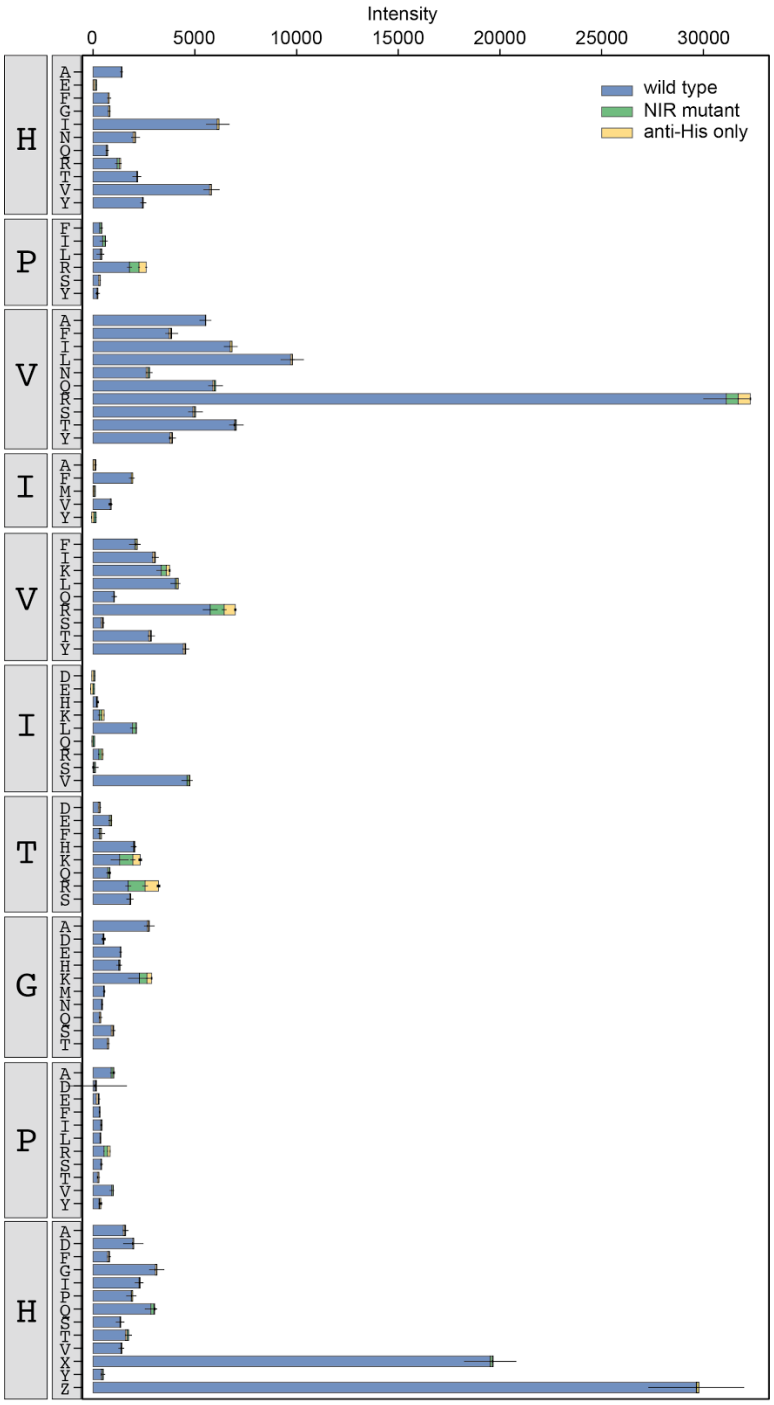

Figure S17. Binding intensity comparisons for PVIVIT library. Measured intensities for WT CN (blue), antibody alone (yellow), and a CN mutant defective in PxIxIT recognition (NIR, green) interacting with PVIVIT library peptides.

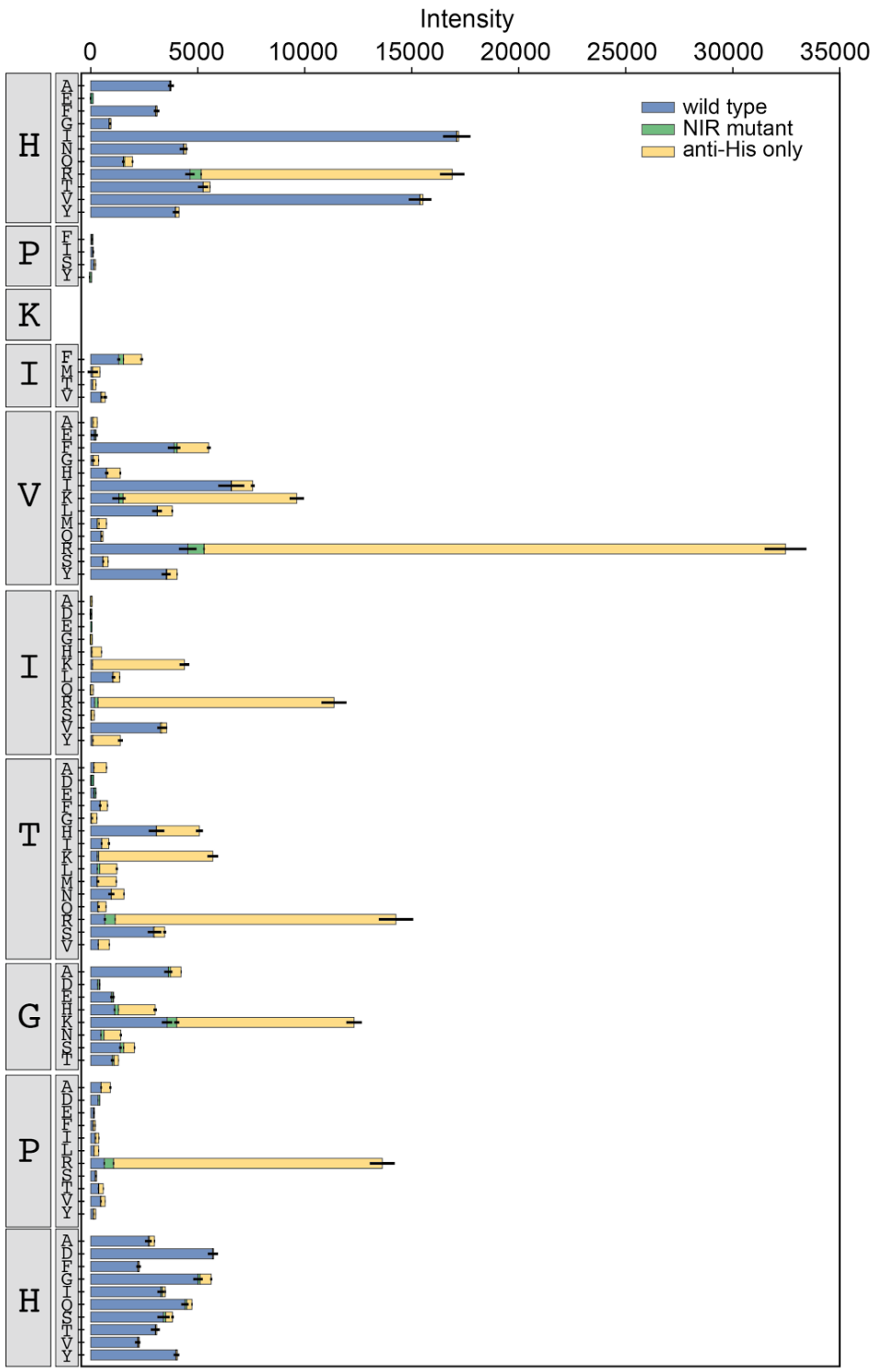

Figure S18. Binding intensity comparisons in PKIVIT library. Measured intensities for WT CN (blue), antibody alone (yellow), and a CN mutant defective in PxIxIT recognition (NIR, green) interacting with PKIVIT library peptides.

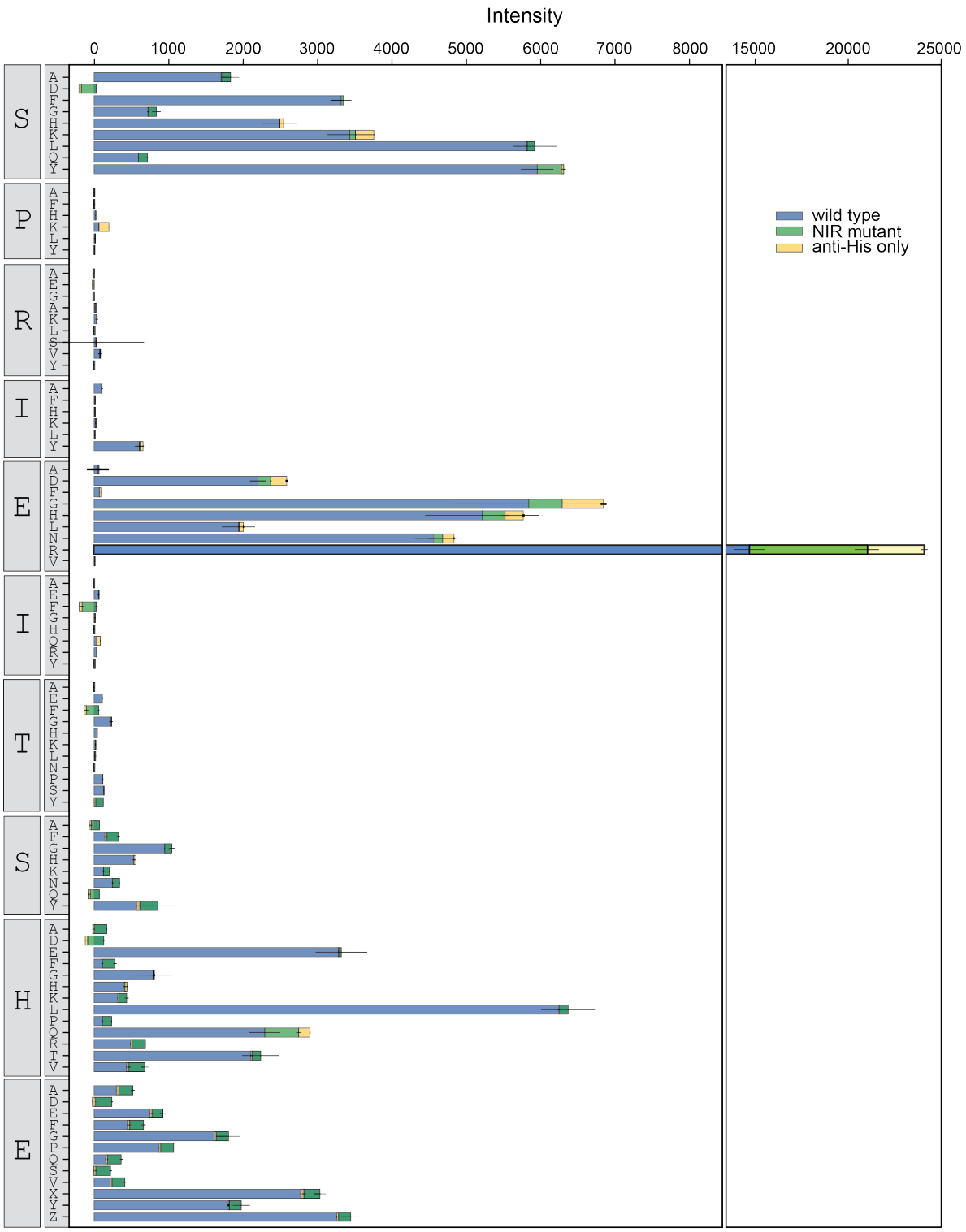

Figure S19. Binding intensity comparisons in NFATc2 library. Measured intensities for WT CN (blue), antibody alone (yellow), and a CN mutant defective in PxIxIT recognition (NIR, green) interacting with NFATc2 library peptides.

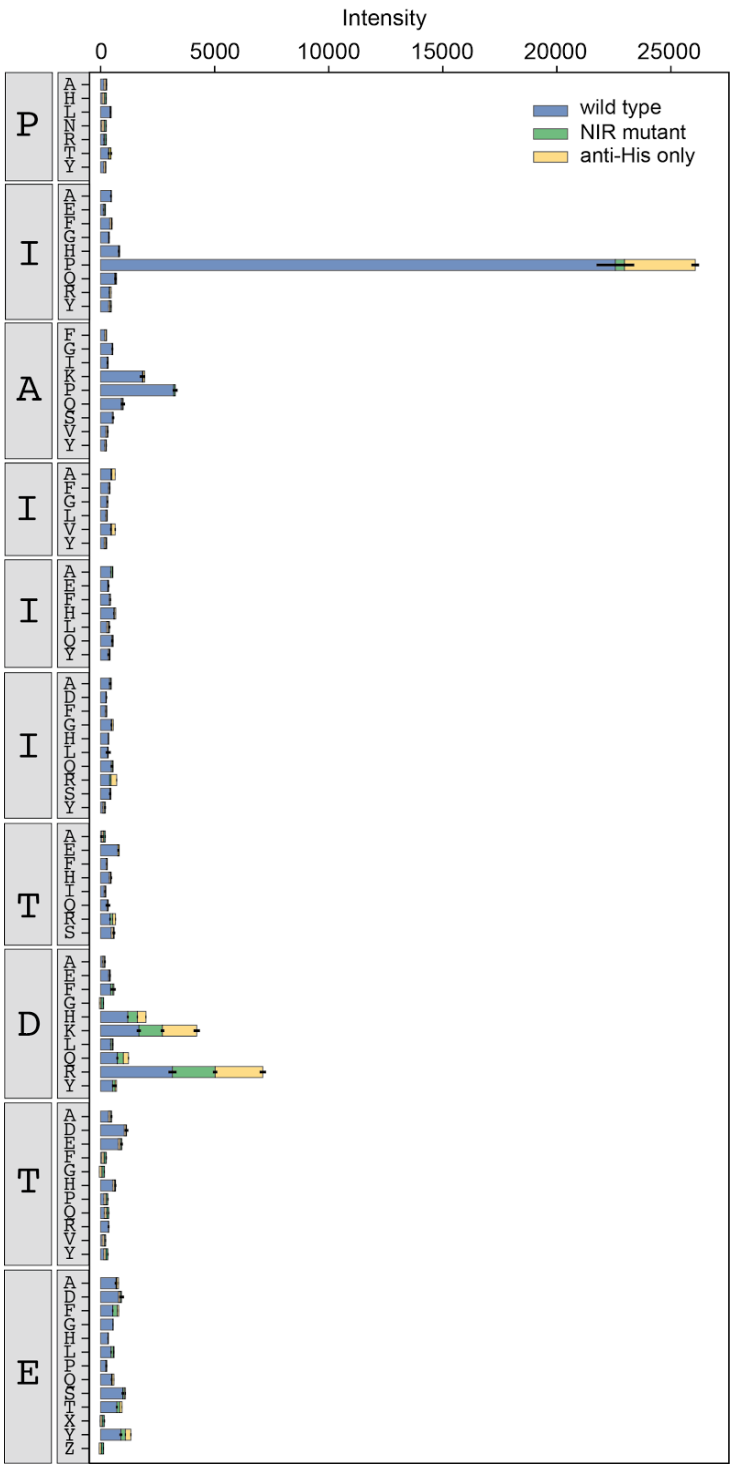

Figure S20. Binding intensity comparisons in AKAP79 library. Measured intensities for WT CN (blue), antibody alone (yellow), and a CN mutant defective in PxIxIT recognition (NIR, green) interacting with PVIVIT library peptides.

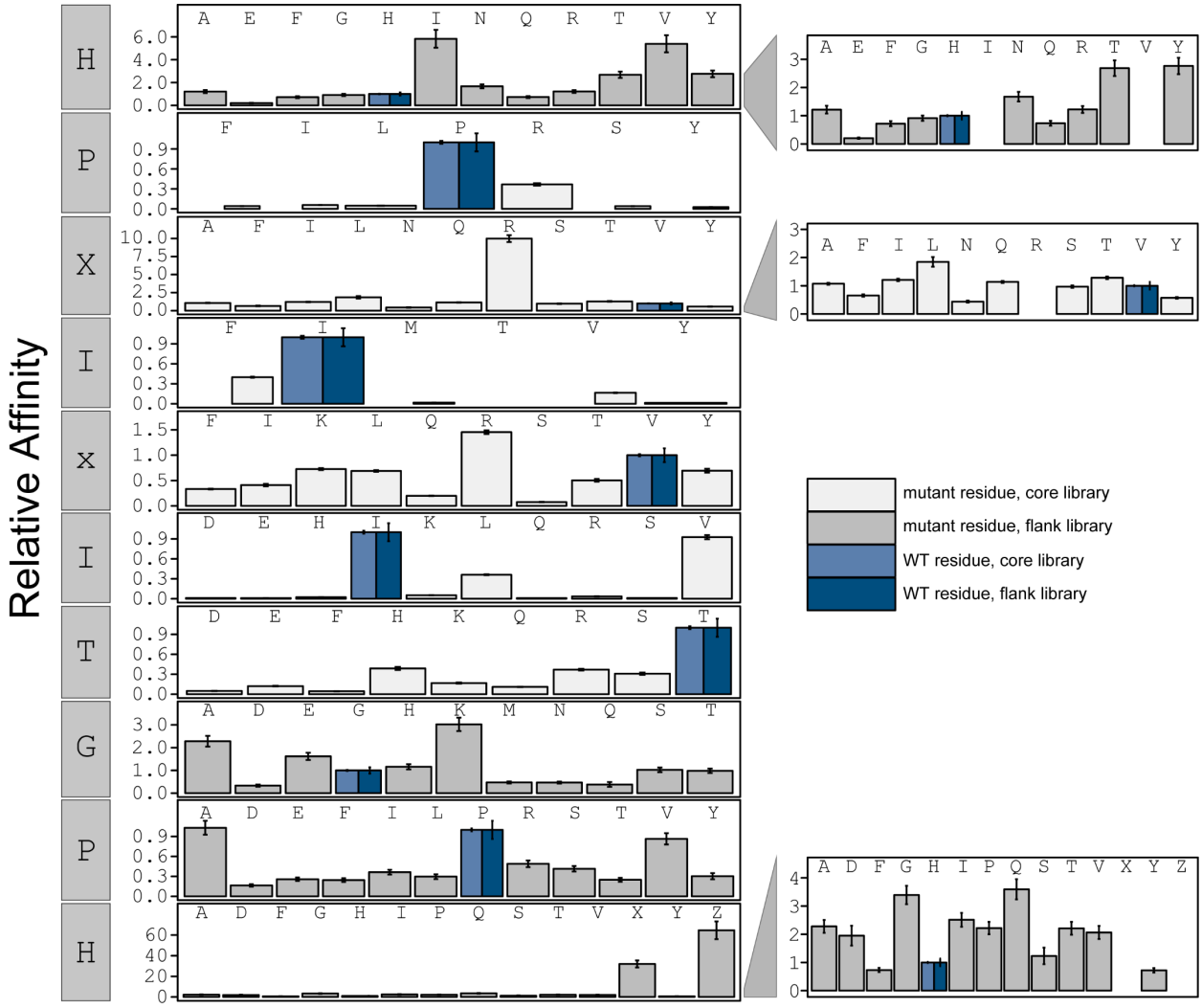

Figure S21. Bar graphs showing PVIVIT specificity. Relative affinity was calculated by normalizing all binding affinity (K_a) to WT binding affinity (light blue: core, dark blue: flank). Phosphoserine and phosphothreonine are represented by 'X' and 'Z', respectively.

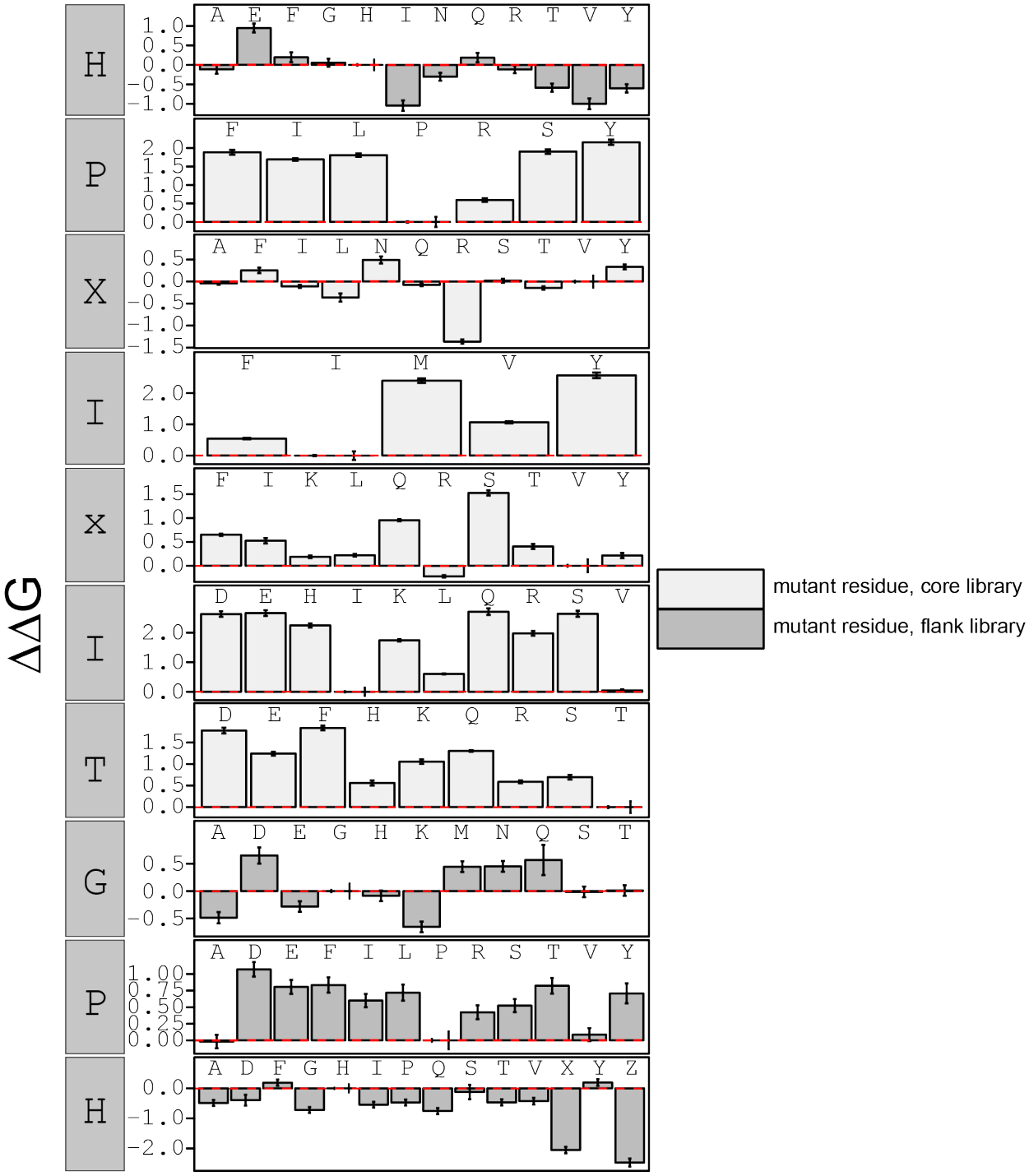

Figure S22. Bar graphs showing PVIVIT specificity. ΔΔG calculated in reference to PxIxIT WT (HPVIVITGPH). Phosphoserine and phosphothreonine are represented by 'X' and 'Z', respectively.

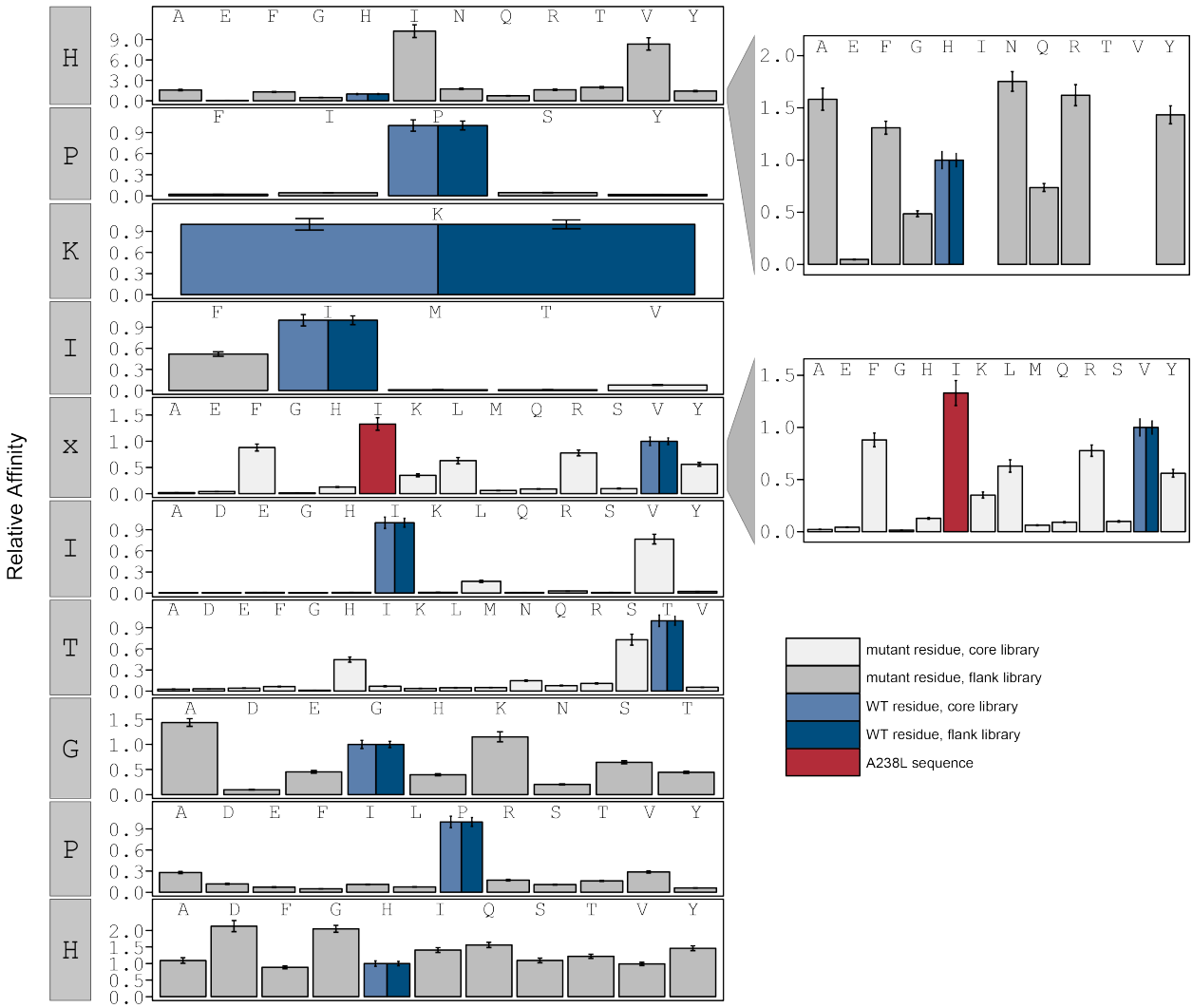

Figure S23. Bar graphs showing PKIVIT specificity. Relative affinity was calculated by normalizing all binding affinity (K_a) to WT binding affinity (light blue: core, dark blue: flank). Peptide sequence AGPH**PKIIIT**GPHEE (red) contains a PxIxIT motif similar to the A238L viral inhibitor.

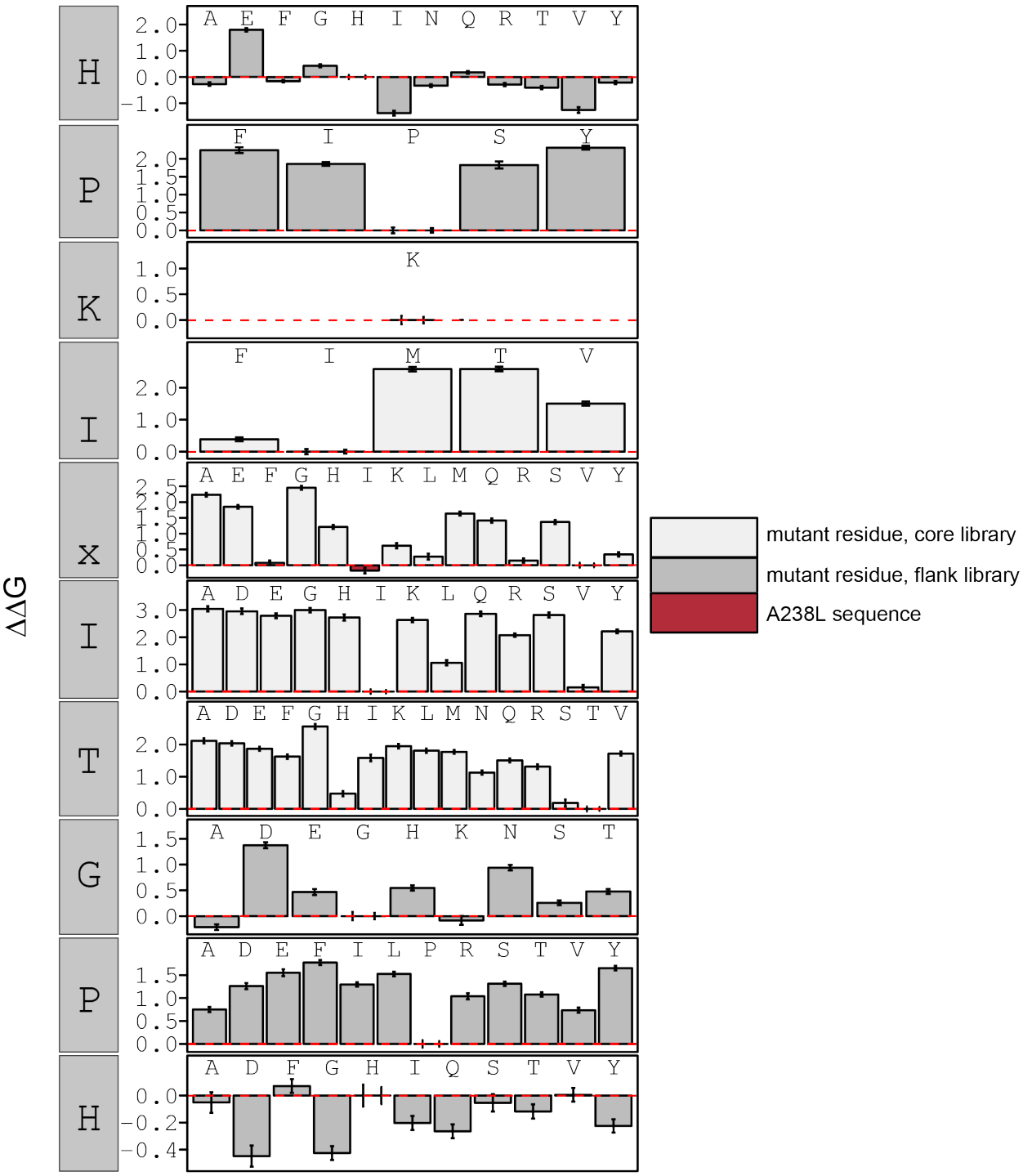

Figure S24. Bar graphs showing PKIVIT specificity. ΔΔG calculated in reference to PKIVIT WT. Peptide sequence AGPH**PKIIIT**GPHEE (red) contains a PxIxIT motif similar to the A238L viral inhibitor.

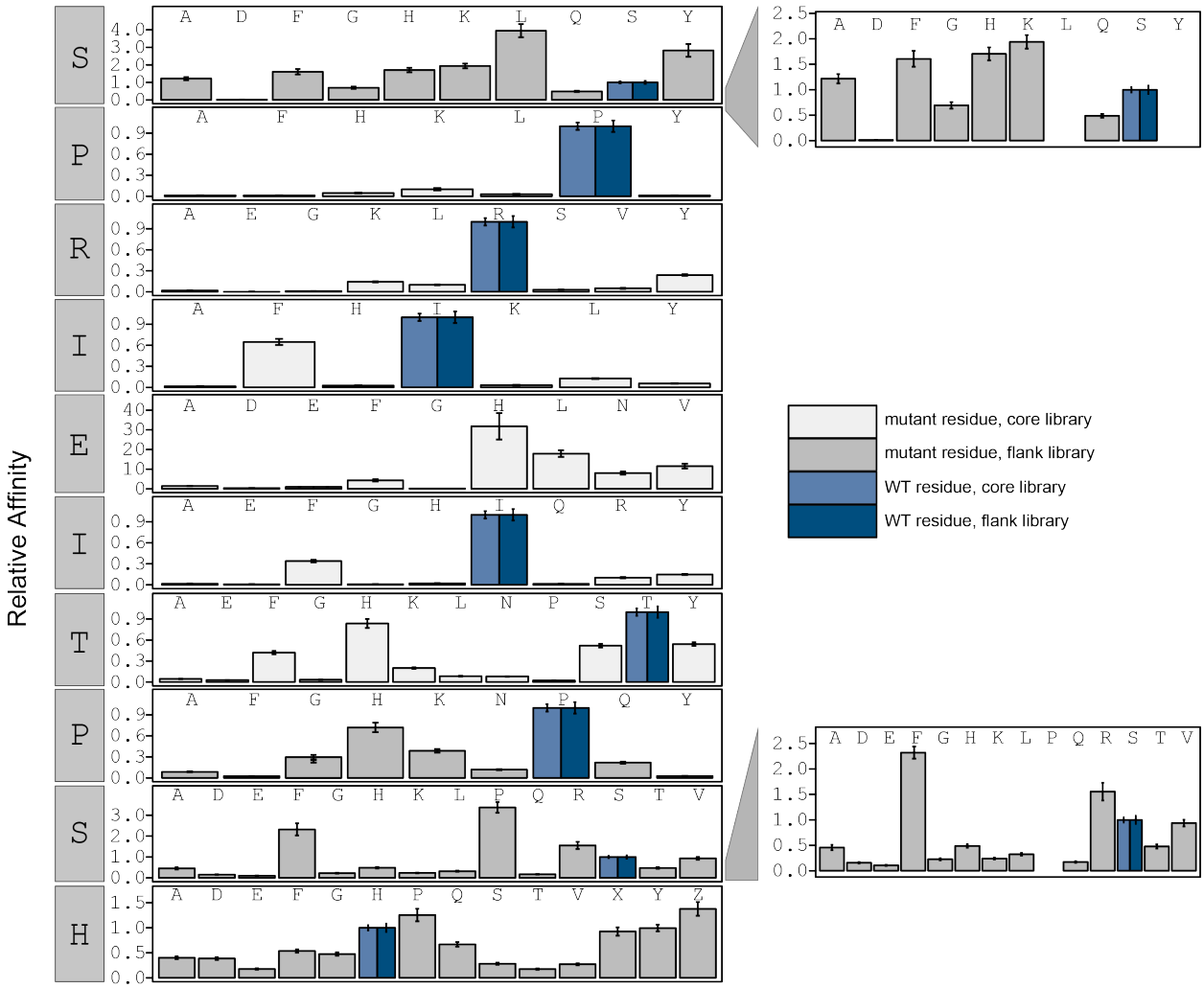

Figure S25. Bar graphs showing NFATc2 specificity. Relative affinity was calculated by normalizing all binding affinity (K_a) to WT (SPRIEITPSH) binding affinity (light blue: core, dark blue: flank). Phosphoserine and phosphothreonine are represented by 'X' and 'Z', respectively.

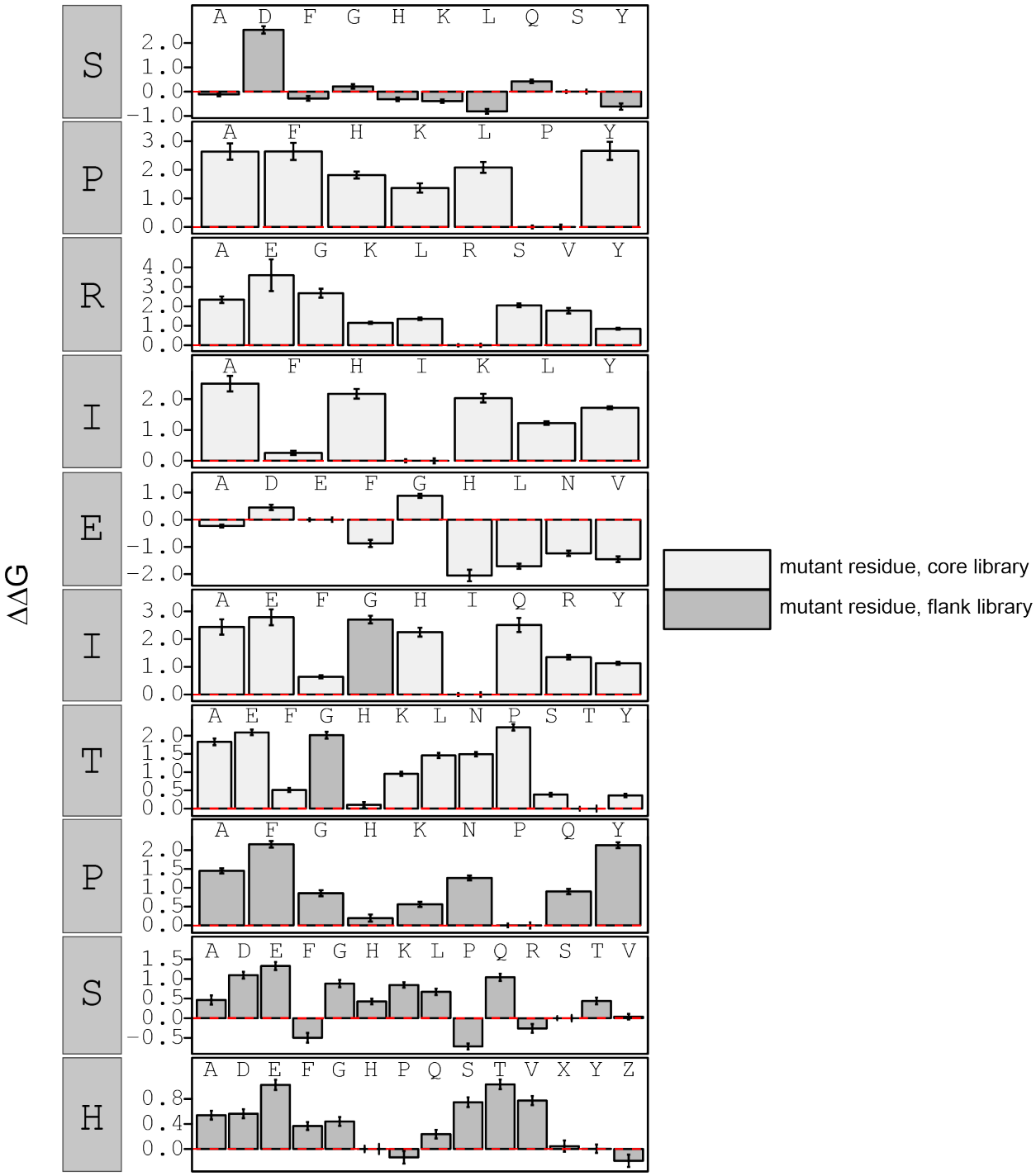

Figure S26. Bar graphs showing NFATc2 specificity. ΔΔG calculated in reference to WT peptide (SPRIEITPSH). Phosphoserine and phosphothreonine are represented by 'X' and 'Z', respectively.

.

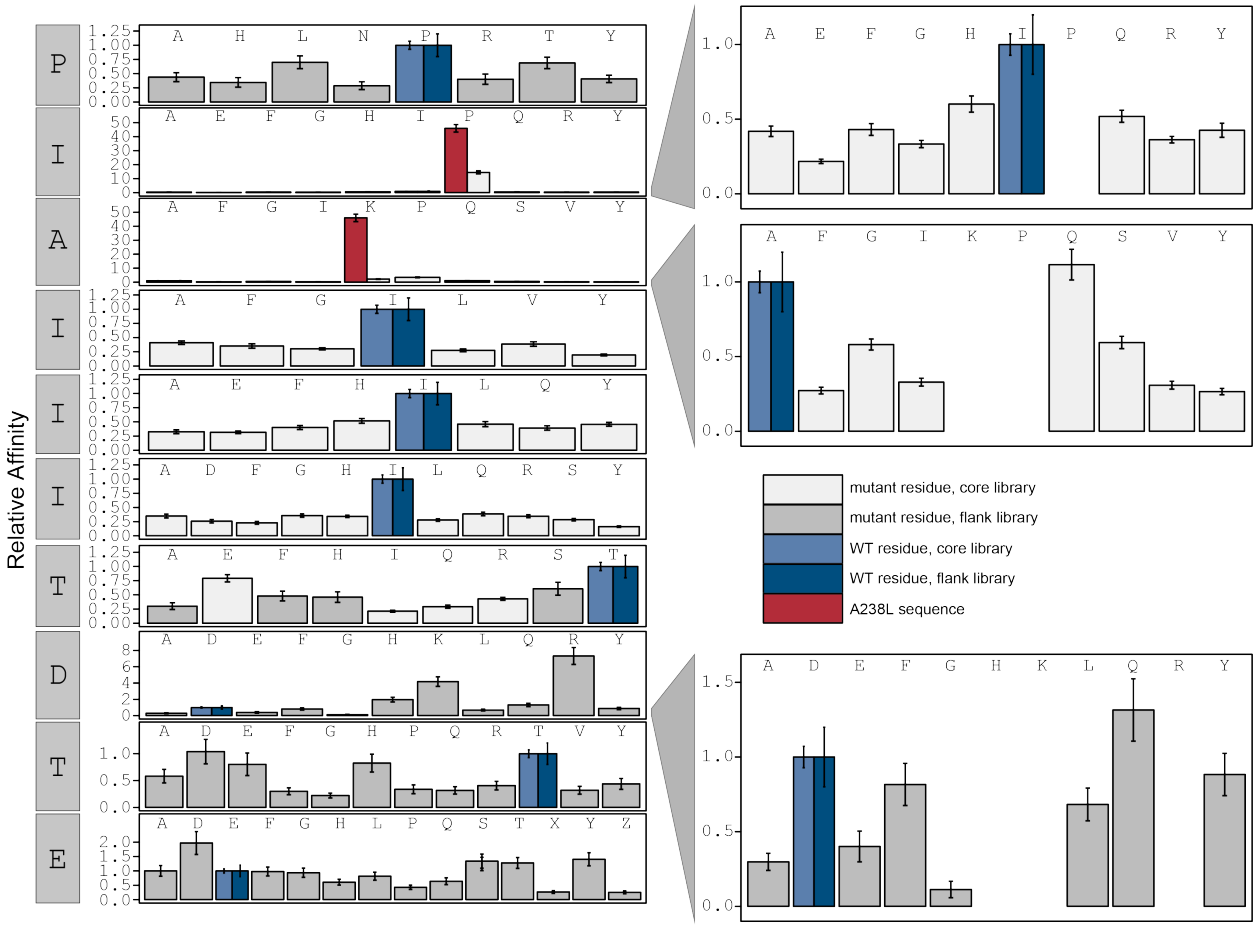

Figure S27. Bar graphs showing AKAP79 specificity. Relative affinity was calculated by normalizing to peptides KRMEPIAIIITDTEIS. Peptide sequence KRME**PKIIIT**TDTEIS (red) contains a PxIxIT motif equivalent to the A238L viral inhibitor. Phosphoserine and phosphothreonine are represented by 'X' and 'Z', respectively.

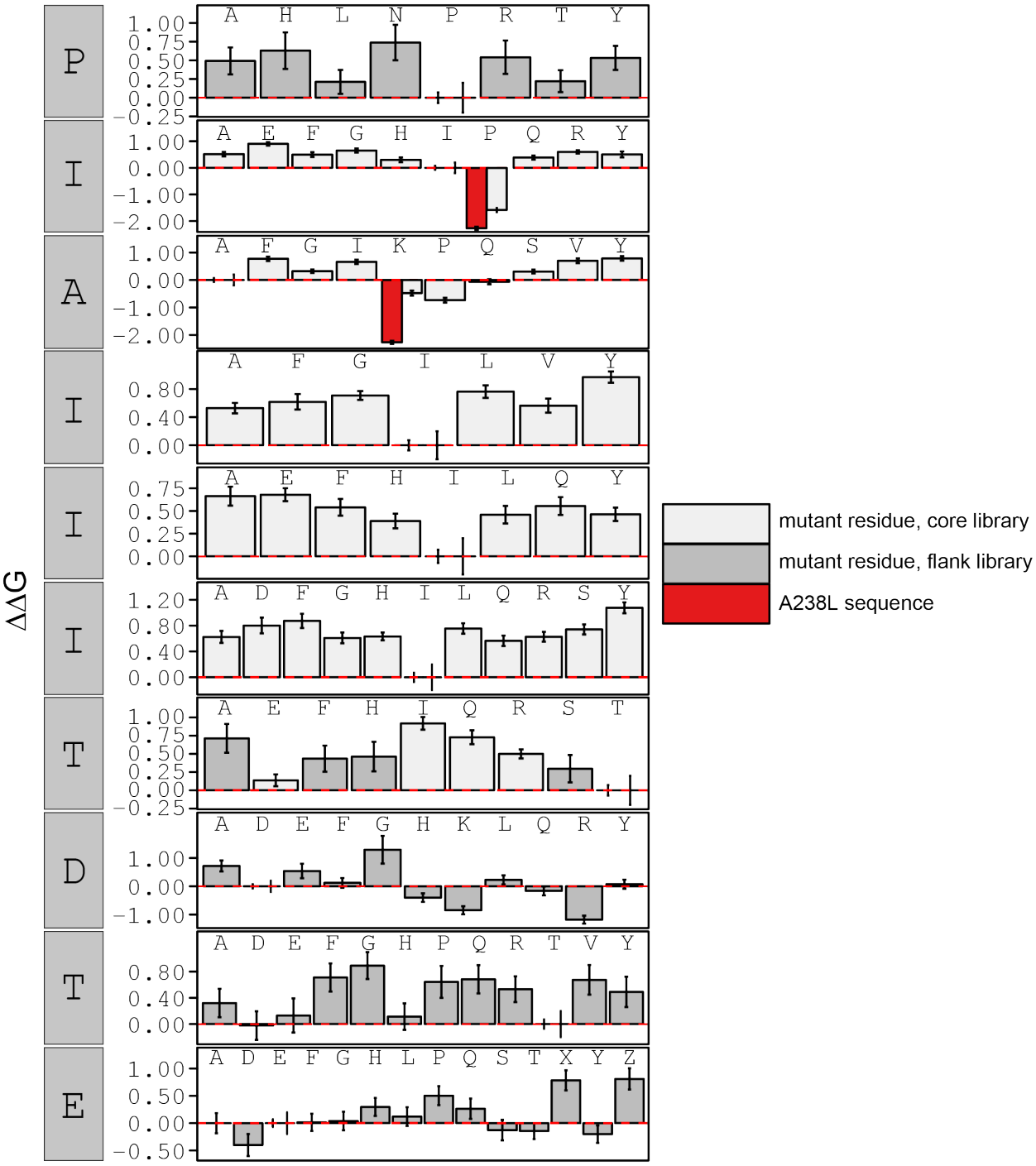

Figure S28. Bar graphs showing AKAP79 specificity. ΔΔG calculated in reference to peptides KRMEPIAIIITDTEIS. Peptide sequence KRME**PKIIIT**TDTEIS (red) contains a PxIxIT motif equivalent to the A238L viral inhibitor. Phosphoserine and phosphothreonine are represented by 'X' and 'Z', respectively.

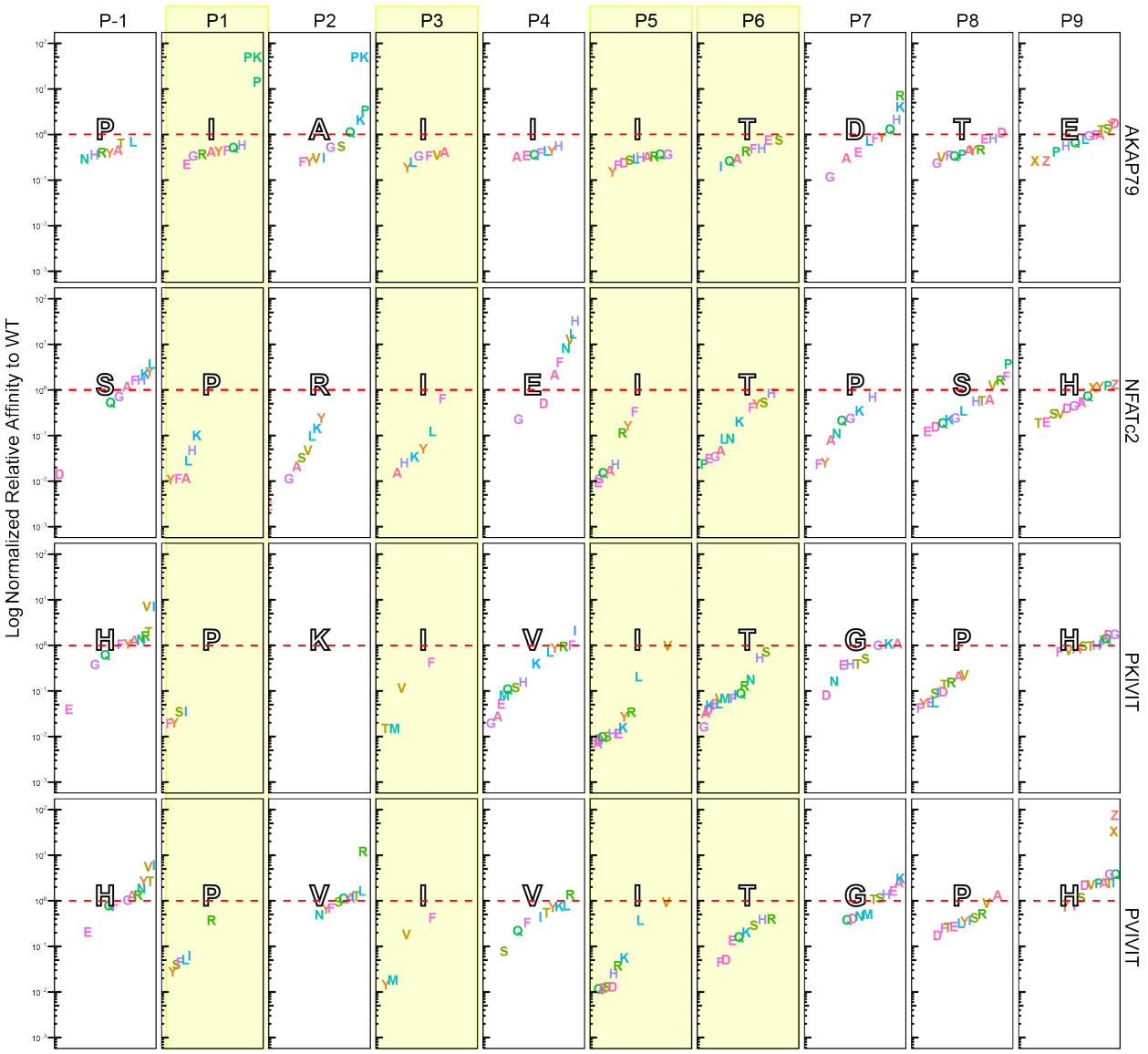

Figure S29. Log K_a normalized to corresponding WT sequences. Amino acid substitutions (single letter code) for all four scaffolds: PVIVIT, PKIVIT, NFATc2, and AKAP79. Positions P-1 to P9 are separated by columns and columns highlighted in yellow represents conserved positions from PxIxIT binding motif. Letters in large black-outlined text corresponds to the WT sequence for that scaffold. Red dotted line is relative affinity = 1. Phosphoserine and phosphothreonine are represented by 'X' and 'Z', respectively.

Figure S30. LogoMaker logos for binding data. Top: binding preferences for AKAP79 (left), NFATc2 (middle left), PKIVIT (middle right), and PVIVIT (right) represented as logos. Scale bar indicates a change in binding affinity of ~ 1 kcal/mol; amino acids are arranged top-to-bottom in order of binding preference. Wild-type residues are shown in red; other residues are shown in grey. **Bottom**: Logos display residues not tested experimentally at each position to illustrate missing data.

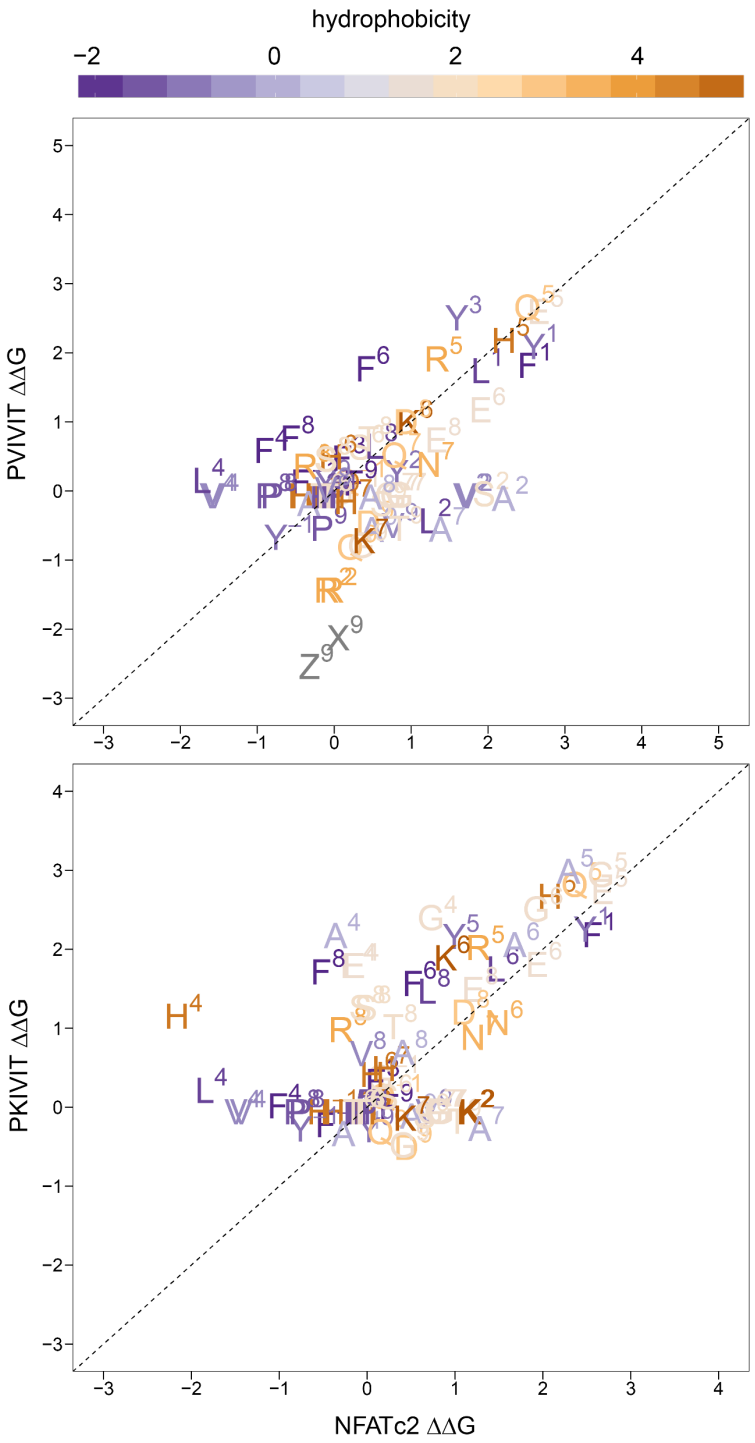

Figure S31. Context-dependent differences in effects of mutations. Measured changes in binding affinity for mutations in PVIVIT (top panel) and PKIVIT (bottom panel) relative to the same mutations in the NFATc2 (PRIEIT) library. Amino acid substitutions are colored according to hydrophobicity with the position of the substitution indicated.

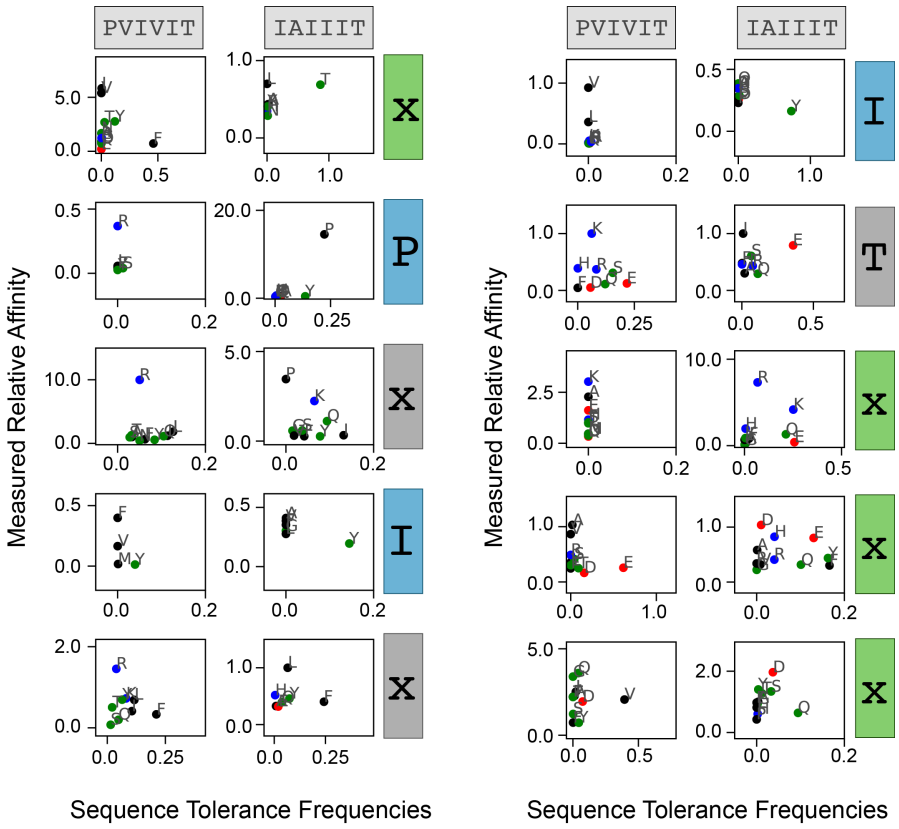

Figure S32. Correlation between measured relative affinity and Backrub-predicted amino acid frequency for each substitution as a function of position. Residues are colored by biochemical properties (red = acidic, blue = basic, black = hydrophobic, green = all other residues).

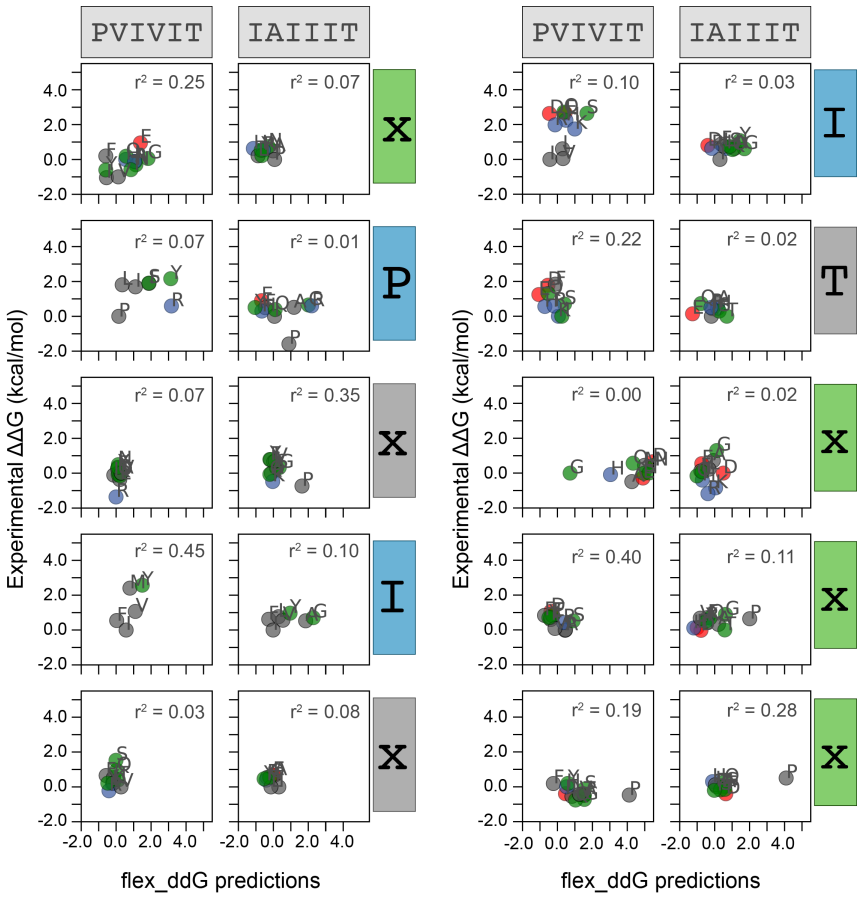

Figure S33. Correlation between measured and predicted change in Gibbs free energy for each mutation at each position within PVIVIT and AKAP79 peptides. Each panel includes calculated correlation coefficients between MRBLE-pep measured changes in binding affinity (*y* axis) and Rosetta-predicted changes in binding affinity (*x* axis). Residues are colored by biochemical properties (red = acidic, blue = basic, black = hydrophobic, green = all other residues).

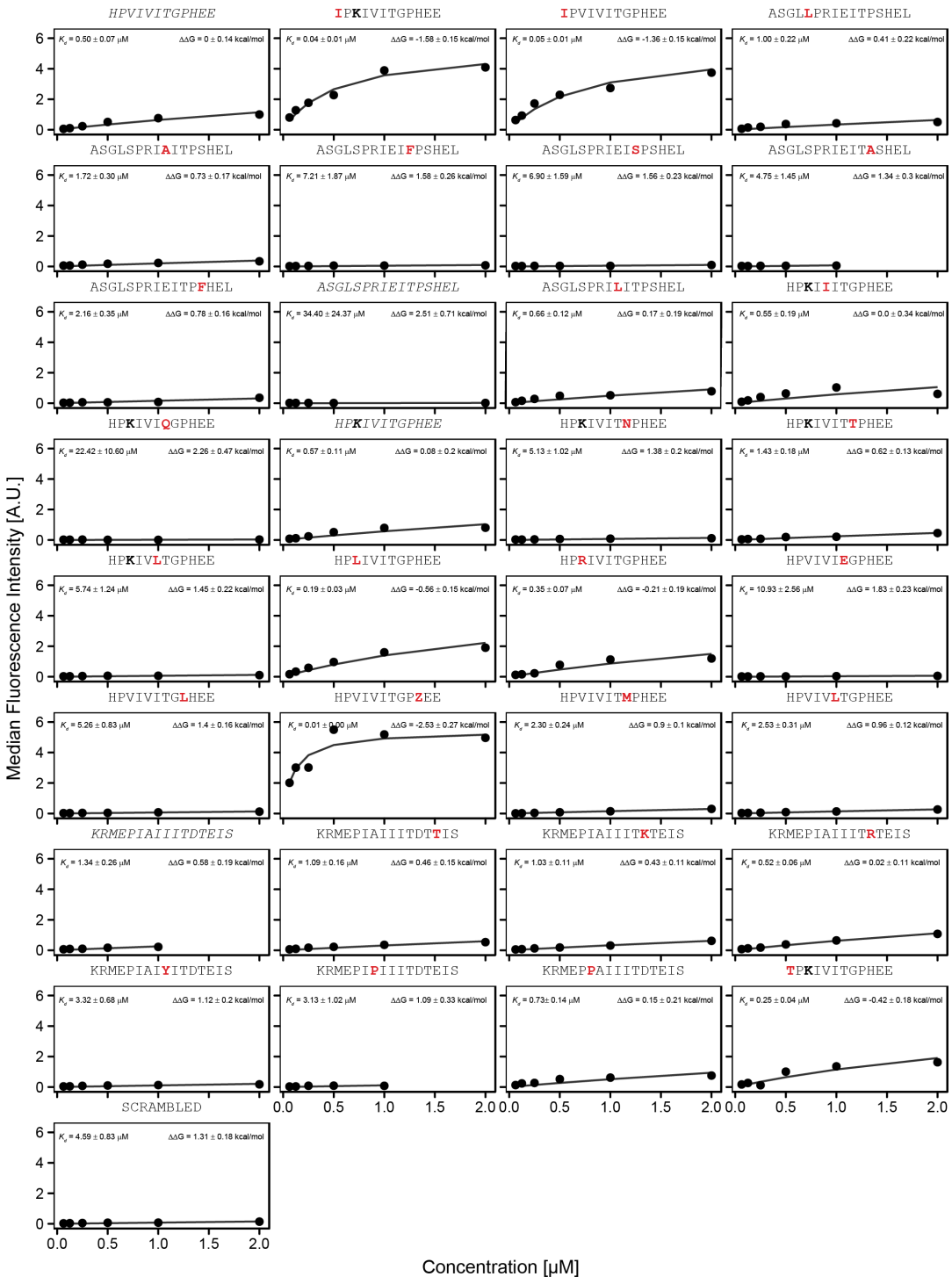

Figure S34. Calibration peptide library, replicate #1. Concentration-dependent binding measurements for selected peptides within the 'calibration' library. For each sequence, measured change in binding affinity relative to the wild-type PVIVIT sequence was determined by a global fit to a single-site binding model (black line); K_d values were calculating from this ΔΔG and the known literature K_d for PVIVIT (0.5 μM)[10].

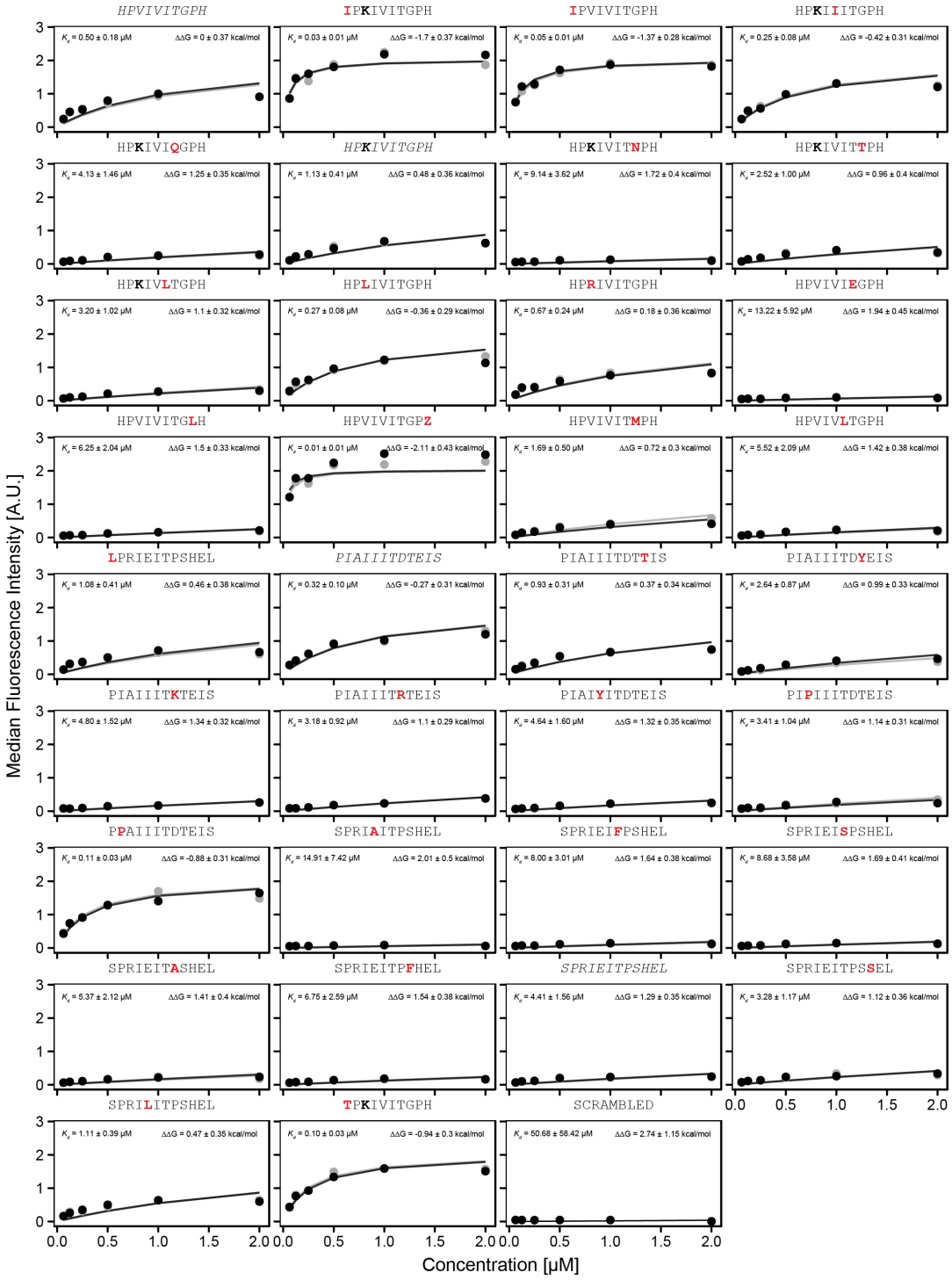

Figure S35. Calibration peptide library, replicate #2. Concentration-dependent binding measurements for selected peptides within the 'calibration' library. For each sequence, measured change in binding affinity relative to the wild-type PVIVIT sequence was determined by a global fit to a single-site binding model (black line); K_d values were calculating from this ΔΔG and the known literature K_d for PVIVIT (0.5 μM).

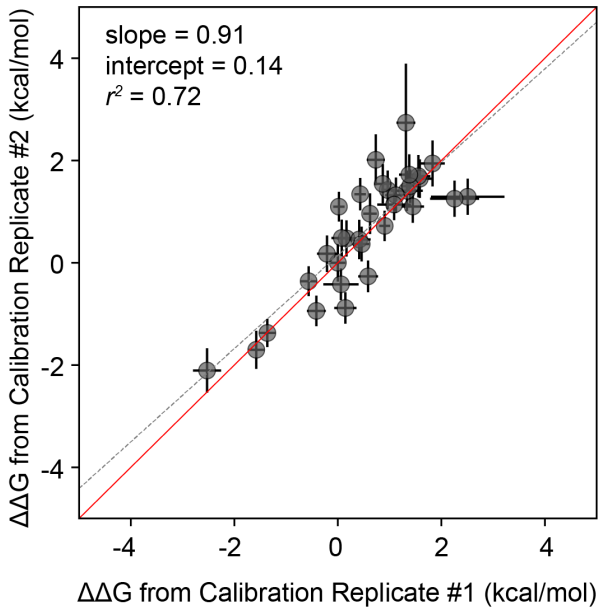

Figure S36. Correlation between ΔΔG measurements for technical replicates of 'calibration' libraries. Correlation between measured ΔΔG values for a full technical replicate (new bead synthesis, new peptide synthesis, and new calcineurin protein purification) for the "calibration" library. Solid red line shows expected 1:1 linear relationship, dotted grey line shows linear regression of log-transformed values.

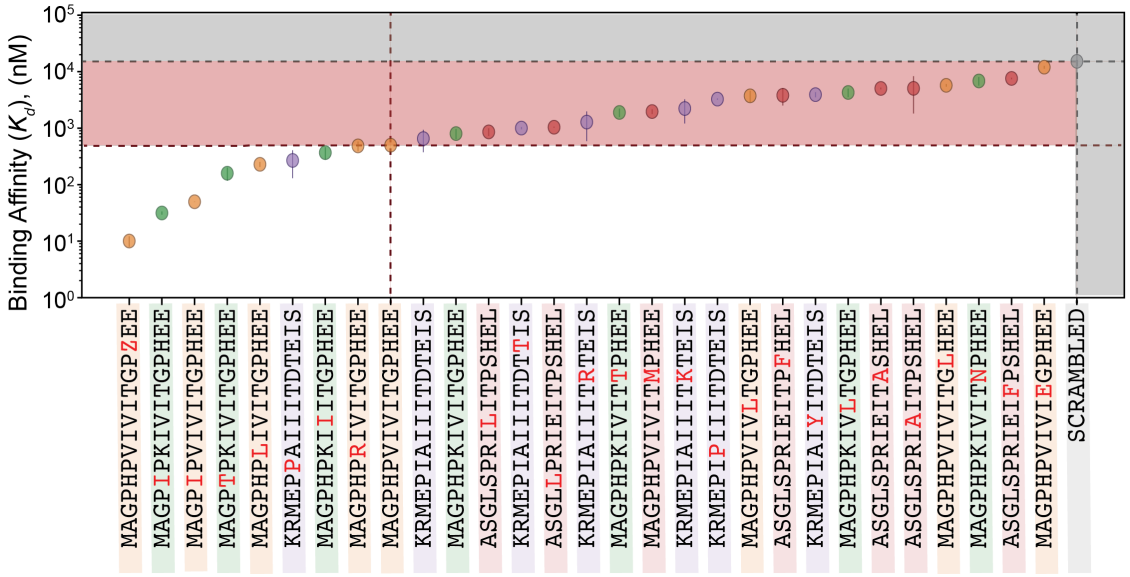

Figure S37. *Kd* values for all peptides within calibration library. PVIVIT variants are shown in orange, PKIVIT variants are shown in green, NFATc2 variants are shown in red, and AKAP79 variants are shown in purple. Values are calculated using the average ΔΔG value relative to PVIVIT for two technical replicates (Figs. S33 and S34) and the literature K_d for PVIVIT (0.5 μM).

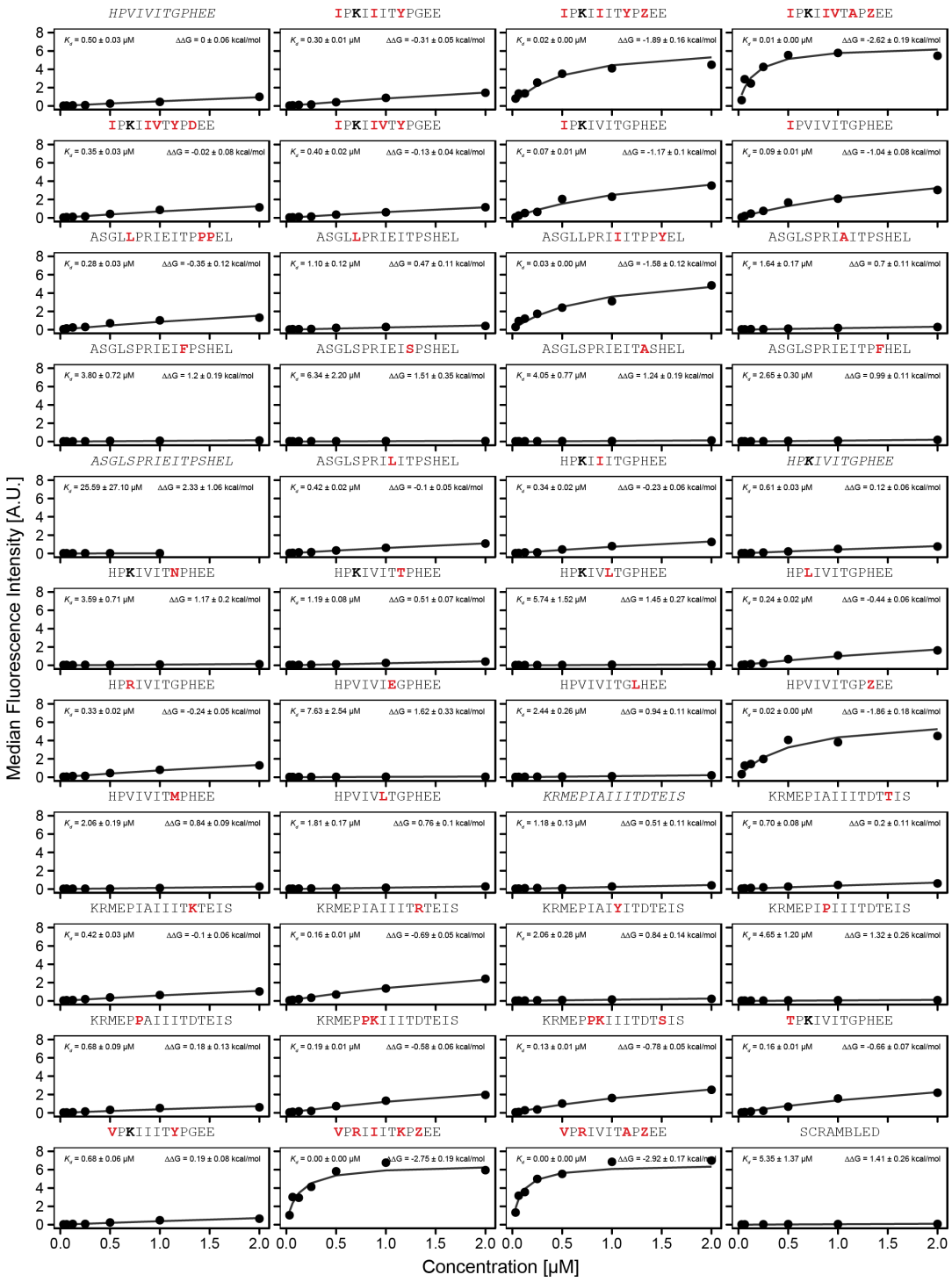

Figure S38. Full calibration library replicate #1. Concentration-dependent binding measurements for selected peptides within the 'full calibration' library. For each sequence, measured change in binding affinity relative to the PVIVIT sequence was determined by a global fit to a single-site binding model (black line); K_d values were calculating from this ΔΔG and the known literature K_d for PVIVIT (0.5 μM).

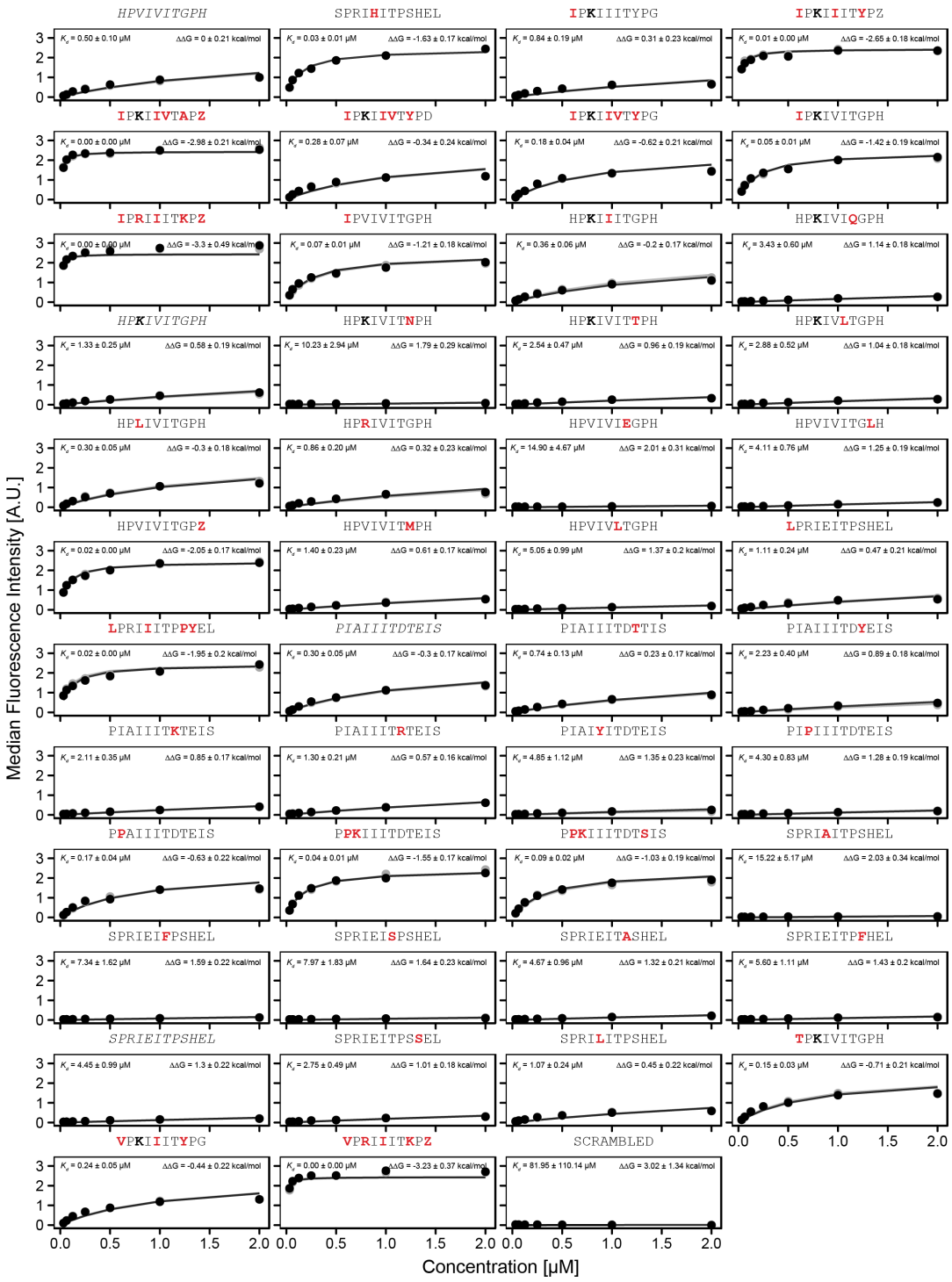

Figure S39. Full calibration library replicate #2. Concentration-dependent binding measurements for selected peptides within the 'full calibration' library. For each sequence, measured change in binding affinity relative to the PVIVIT sequence was determined by a global fit to a single-site binding model (black line); K_d values were calculating from this ΔΔG and the known literature K_d for PVIVIT (0.5 μM).

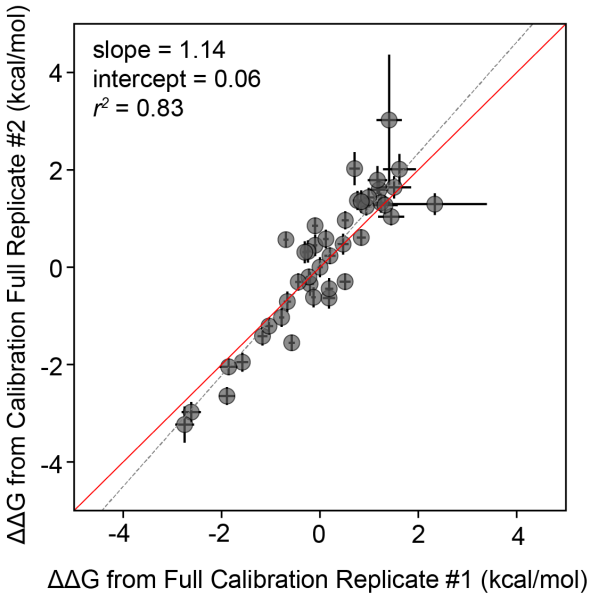

Figure S40. Correlation between ΔΔG measurements for technical replicates of full calibration libraries. Correlation between measured ΔΔG values for a full technical replicate (new bead synthesis, new peptide synthesis, and new calcineurin protein purification) for the "full calibration" library. Solid red line shows expected 1:1 linear relationship, dotted grey line shows linear regression of log-transformed values.

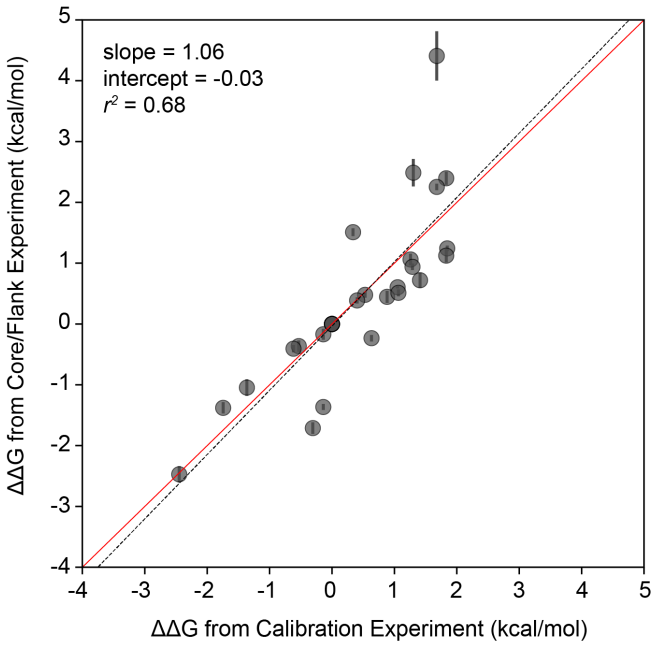

Figure S41. Correlation between ΔΔG measurements for core/flank library measurements and "calibration" library measurements. Solid red line shows expected 1:1 linear relationship, dotted grey line shows linear regression of log-transformed values.

References

1. Park, S., Uesugi, M. & Verdine, G. L. A second calcineurin binding site on the NFAT regulatory domain. *Proc. Natl. Acad. Sci.* **97,** 7130–7135 (2000).
2. Garcia-Cozar, F. J. *et al.* Two-site interaction of nuclear factor of activated T cells with activated calcineurin. *J. Biol. Chem.* **273,** 23877–23883 (1998).
3. Mulero, M. C. *et al.* Inhibiting the Calcineurin-NFAT (Nuclear Factor of Activated T Cells) Signaling Pathway with a Regulator of Calcineurin-derived Peptide without Affecting General Calcineurin Phosphatase Activity. *J. Biol. Chem.* **284,** 9394–9401 (2009).
4. Sieber, M. & Baumgrass, R. Novel inhibitors of the calcineurin/NFATc hub - alternatives to CsA and FK506? *Cell Commun. Signal.* **7,** 25 (2009).
5. Li, H., Rao, A. & Hogan, P. G. Interaction of calcineurin with substrates and targeting proteins. *Trends Cell Biol.* **21,** 91–103 (2011).
6. Grigoriu, S. *et al.* The Molecular Mechanism of Substrate Engagement and Immunosuppressant Inhibition of Calcineurin. *PLoS Biol.* **11,** e1001492 (2013).
7. Li, H., Rao, A. & Hogan, P. G. Structural Delineation of the Calcineurin–NFAT Interaction and its Parallels to PP1 Targeting Interactions. *J. Mol. Biol.* **342,** 1659–1674 (2004).
8. Li, H., Zhang, L., Rao, A., Harrison, S. C. & Hogan, P. G. Structure of Calcineurin in Complex with PVIVIT Peptide: Portrait of a Low-affinity Signalling Interaction. *J. Mol. Biol.* **369,** 1296–1306 (2007).
9. Gill, H. S., Roush, E. D., Dutcher, L. & Patel, S. Direct Evidence for Calcineurin Binding to the Exon-7 Loop of the Sodium-Bicarbonate Cotransporter NBCn1. *Int. J. Biol. Sci.* **10,** 771–776 (2014).
10. Aramburu, Jose *et al.* Affinity-Driven Peptide Selection of an NFAT Inhibitor More Selective Than Cyclosporin A. *Science* **285,** 2129–2133 (1999).
11. Aramburu, J. *et al.* Selective inhibition of NFAT activation by a peptide spanning the calcineurin targeting site of NFAT. *Mol. Cell* **1,** 627–637 (1998).
12. Ma, Y. *et al.* Enzymatic and thermodynamic analysis of calcineurin inhibition by RCAN1. *Int. J. Biol. Macromol.* **72,** 254–260 (2015).
13. Liu, R., Marik, J. & Lam, K. S. A Novel Peptide-Based Encoding System for "One-Bead One-Compound" Peptidomimetic and Small Molecule Combinatorial Libraries. *J. Am. Chem. Soc.* **124,** 7678–7680 (2002).